

CB2-Selective Cannabinoid Receptor Ligands: Synthesis, Pharmacological Evaluation, and Molecular Modeling Investigation of 1,8-Naphthyridin-2(1H)-one-3-carboxamides

Valentina Lucchesi,[†] Dow P. Hurst,[‡] Derek M. Shore,[‡] Simone Bertini,[†] Brandie M. Ehrmann,[‡] Marco Allarà,[§] Lyle Lawrence,[‡] Alessia Ligresti,[§] Filippo Minutolo,[†] Giuseppe Saccomanni,[†] Haleli Sharir,^{||} Marco Macchia,[†] Vincenzo Di Marzo,[§] Mary E. Abood,^{||} Patricia H. Reggio,^{*,‡} and Clementina Manera^{*,†}

[†]Dipartimento di Farmacia, Università di Pisa, Via Bonanno 6, 56126 Pisa, Italy

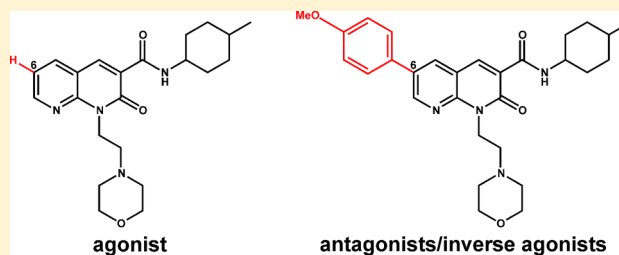
[‡]Center for Drug Discovery, University of North Carolina Greensboro, Greensboro, North Carolina 27402, United States

[§]Endocannabinoid Research Group, Istituto di Chimica Biomolecolare, Consiglio Nazionale delle Ricerche, Via Campi Flegrei 34, 80078 Pozzuoli, Napoli, Italy

^{||}Center for Substance Abuse Research, Temple University, Philadelphia, Pennsylvania 19140, United States

S Supporting Information

ABSTRACT: We have recently identified 1,8-naphthyridin-2(1H)-one-3-carboxamide as a new scaffold very suitable for the development of new CB2 receptor potent and selective ligands. In this paper we describe a number of additional derivatives in which the same central scaffold has been variously functionalized in position 1 or 6. All new compounds showed high selectivity and affinity in the nanomolar range for the CB2 receptor. Furthermore, we found that their functional activity is controlled by the presence of the substituents at position C-6 of the naphthyridine scaffold. In fact, the introduction of substituents in this position determined a functionality switch from agonist to antagonists/inverse agonists. Finally, docking studies showed that the difference between the pharmacology of these ligands may be in the ability/inability to block the Toggle Switch W6.48(258) (χ_1 $g^+ \rightarrow trans$) transition.



■ INTRODUCTION

Cannabinoids are a unique family of terpenophenolic active constituents of *Cannabis sativa*; Δ^9 -tetrahydrocannabinol (THC) is the most relevant member, owing to its psychoactive effects and a wide variety of pharmacological effects.^{1,2} The isolation and characterization of THC³ allowed for the identification of two distinct cannabinoid receptors (CBRs), named CB1 receptor (CB1R) and CB2 receptor (CB2R), that have been cloned and characterized from mammalian tissues.^{4,5} CB1R is abundantly expressed in the central nervous system (CNS), with the highest densities in the hippocampus, cerebellum, and striatum.⁶ Locations outside the brain have also been indicated, including adipose tissue, liver, muscle, the gastrointestinal tract, pancreas, urinary bladder, lung, heart, adrenal gland, testis, uterus, and prostate.^{7–10} In contrast, CB2R has been reported to be essentially limited to the cells associated with the immune system, such as spleen, thymus, and tonsils,⁵ but it also has been found in low concentrations in the brain.¹¹

Since the discovery of the CBRs and their endogenous ligands, numerous studies implicate the endocannabinoid system in several physiological and pathological processes, including cancer, appetite, fertility, memory, neuropathic and

inflammatory pain, obesity, and neurodegenerative disease.¹² At the present time, CB2R has gained attention as a potential target for immunoregulation. Recent advances suggest a role for CB2R within the nervous system, particularly in inflammatory conditions such as neurodegenerative disease (Parkinson's disease, Alzheimer's disease, Huntington's disease, multiple sclerosis, etc.), since CB2R is up-regulated in the brain under these conditions and disease states. This finding is supported by observing the pattern of expression of CB2R during microglia differentiation using an *in vitro* model of multistep activation.^{13–15} Additional data suggest that CB2R-selective agonists show promise for suppressing inflammatory and neuropathic pain states. Behavioral, electrophysiological, and neurochemical studies all support a role for CB2R activation in modulating inflammatory nociception. Moreover, recent reviews have focused on the evidence for the functional neuronal presence and the emerging role of CB2R in neuropsychiatric disorders.^{16,17} Finally, CB2R is overexpressed in several tumor cells, and various *in vitro* studies and animal models have shown

Received: March 31, 2014

Published: October 1, 2014

that activation of the CB2R induces apoptosis, inhibits tumor growth, and inhibits neo-angiogenesis.^{1,18}

The effectiveness of selective CB2R agonists as neuro-protective and anticancer agents prompted us to report our efforts in this field. Our aim was to identify new selective CB2R agonists as potential drugs devoid of the psychotropic side effects associated with CB1R.

Recently we described the synthesis, binding affinities, and pharmacological characterization of a novel series of 1,8-naphthyridin-2(1*H*)-one-3-carboxamides of general structure A (Figure 1), acting as potent and selective CB2R ligands.¹⁹



Figure 1. General structure of compounds A.

Furthermore, the concentration-dependent inhibitory action on human basophils activation and the concentration-dependent decrease of cell viability in Jurkat cells shown by one of these derivatives strongly suggest that these compounds possess agonist properties on CB2R.¹⁹

In an effort to develop improved naphthyridine-based CB2R ligands and also to develop structure–activity relationships (SARs) for both CB1R and CB2R, the present paper describes the synthesis and the pharmacological properties of a number of additional 1,8-naphthyridin-2(1*H*)-one-3-carboxamide derivatives, 1–26 (summarized in Tables 1 and 2, below), in which the central naphthyridine scaffold has been variously functionalized with different substituents in position 1 or 6. The 4-methylcyclohexyl carboxamide group in position 3 has been selected on the basis of binding results obtained for derivatives A. The new compounds were tested in competitive binding assays toward both human recombinant CB1R and CB2R expressed in HEK-293 cells and were found to be selective for CB2R. Furthermore, the functional activity of the most representative compounds was determined by a β -arrestin 2 recruitment assay using U2OS cells co-expressing CB2R and β -arr2/GFP as well as with a forskolin-stimulated cAMP assay, demonstrating that the functionality of tested compounds is controlled by the presence of the substituents at position C-6 of the naphthyridine scaffold.

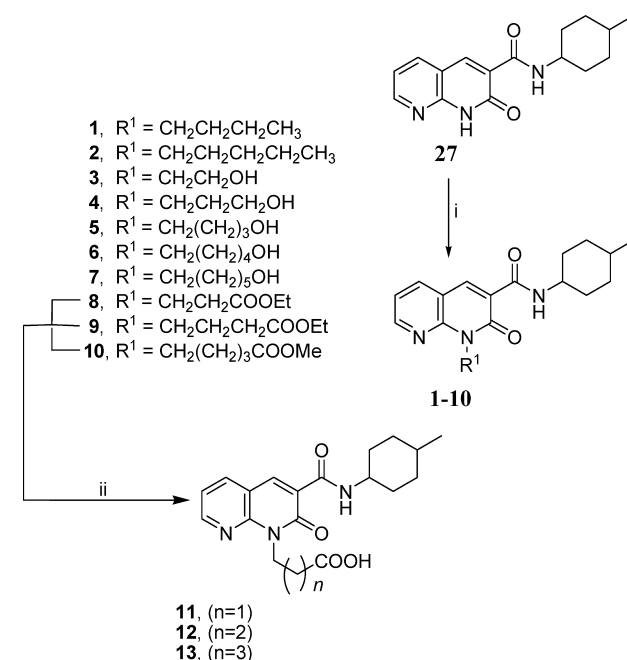
Finally, docking studies were performed in order to analyze both the complex of the CB2R in its inactive state (R) with antagonists/inverse agonists and the complex of the CB2R in its activated state (R*) with agonists. These studies demonstrated that the difference between the pharmacology of these ligands may be in the ability/inability to block the Toggle Switch W6.48(258) (χ 1 *g*+ \rightarrow *trans*) transition.

CHEMISTRY

The synthesis of compounds 1–26 is depicted in Schemes 1–3. As reported in Scheme 1 the N1-alkylation of 1,8-naphthyridine-3-carboxamide 27¹⁹ in anhydrous DMF with the suitable halogenated reagent in the presence of cesium carbonate at 50 °C for 12 h afforded the desired compounds 1–10. The carboxylic acid derivatives 11–13 were obtained from the corresponding esters 8–10 by alkaline hydrolysis followed by acidification.

The synthesis of fluorine derivatives 14–16 is outlined in Scheme 2. Treatment of alcohol derivatives 5–7 with

Scheme 1. Synthesis of 1,8-Naphthyridin-2(1*H*)-one-3-carboxamide Derivatives 1–13^a



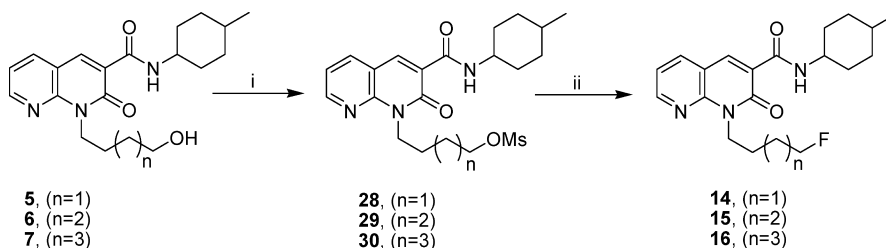
^aReagents and conditions: (i) Cs₂CO₃, R¹Cl or R¹Br, DMF, 50 °C, 12 h, 23%–85%; (ii) NaOH aq. 10%. 110 °C, 5h, 92%–95%.

methanesulfonyl chloride in anhydrous dichloromethane and triethylamine at room temperature for 6 h generated mesylates 28–30. Exposure of 28–30 to tetrabutylammonium fluoride in THF at reflux for 4 h provided derivatives 14–16.

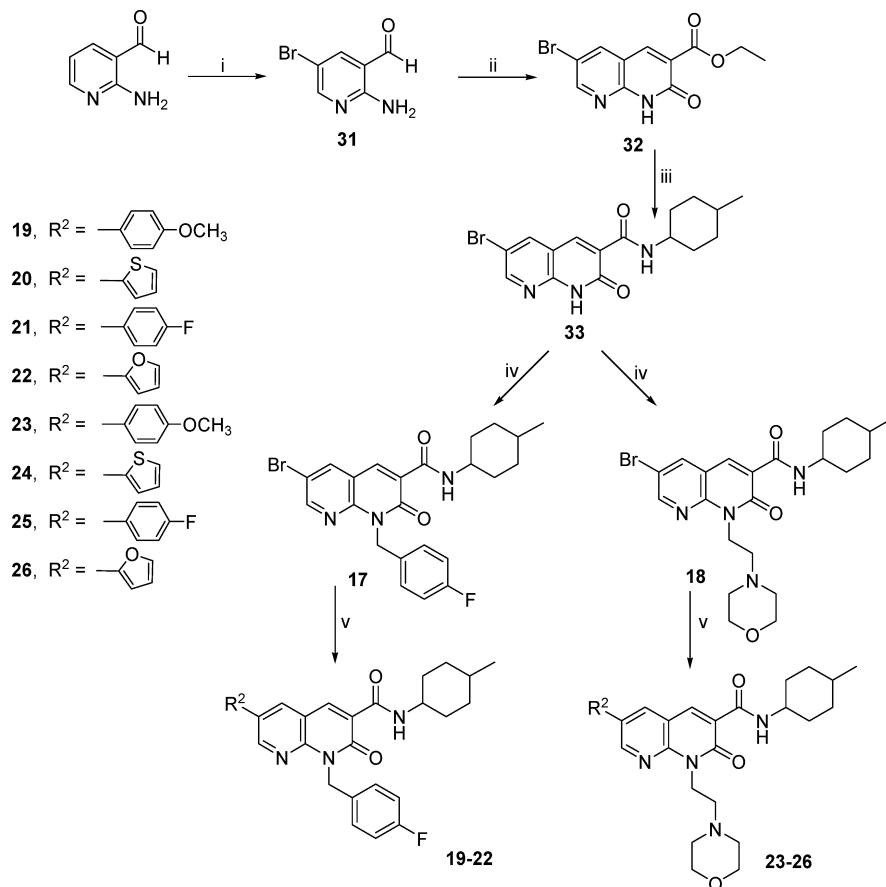
The synthetic route to obtain 6-substituted 1,8-naphthyridin-2(1*H*)-one-3-carboxamide derivatives 17–26 is outlined in Scheme 3. 2-Aminonicotinaldehyde was treated with bromine in glacial acetic acid at room temperature for 24 h to obtain the corresponding 6-bromo derivative 31, which was refluxed with diethyl malonate and in the presence of piperidine in EtOH for 24 h to afford ethyl 6-bromo-1,8-naphthyridin-2(1*H*)-one-3-carboxylate 32. The reaction of ethyl ester 32 with a *cis/trans* diastereoisomeric mixture of 4-methylcyclohexylamine in a sealed tube for 24 h at 150 °C provided the desired carboxamide 33. *N*-Alkylation of 33 in anhydrous DMF with *p*-fluorobenzyl chloride or 4-(2-chloroethyl)morpholine in the presence of cesium carbonate afforded the desired 1,8-naphthyridin-2-one derivatives 17 and 18, respectively. To obtain compounds 19–26, 6-bromo derivatives 17 or 18 were subjected to a cross-coupling reaction with suitable boronic acids in dioxane under Suzuki conditions by generating *in situ* Pd(PPh₃)₄ as the catalyst and aqueous Na₂CO₃ (2 M) as the base. These reactions were carried out in a microwave reactor (CEM). Each crude mixture was purified by flash chromatography. For compounds 17, 20, and 22, the separation of *cis* and *trans* isomers was also obtained.

RESULTS AND DISCUSSION

CB1R and CB2R Affinity. The binding affinities (*K_i* values) of target compounds 1–26 were evaluated by competitive radioligand displacement assays against the human CB1R and CB2R using [³H]CP-55,940 as the radioligand for both receptors.¹⁹ The results are summarized in Tables 1 and 2, together with the *K_i* values of previously reported morpholi-

Scheme 2. Synthesis of 1,8-Naphthyridin-2(1H)-one-3-carboxamide Derivatives 14–16^a

^aReagents and conditions: (i) CH₂Cl₂, Et₃N, MsCl, r.t., 6 h, 37%–86%; (ii) TBAF, CH₂Cl₂, reflux, 4 h, 47%–49%.

Scheme 3. Synthesis of 1,8-Naphthyridin-2(1H)-one-3-carboxamide Derivatives 17–26^a

^aReagents and conditions: (i) Br₂, AcOH, 24 h, r.t., 73%; (ii) diethyl malonate, piperidine, EtOH, reflux, 12 h, 90%; (iii) 4-methylcyclohexylamine, 150 °C, 24 h, 65%; (iv) Cs₂CO₃, *p*-fluorobenzyl chloride or 4-(2-chloroethyl)morpholine, DMF, 50 °C, 12 h, 71%, 92%; (v) Ph₃P, Pd(OAc)₂, dioxane, Na₂CO₃, suitable boronic acid, 150 °C, microwave (200 W, 100 psi, 15 min, under stirring), 41–94%.

noethyl and *p*-fluorobenzyl derivatives **A1** and **A2**, respectively,¹⁹ and reference compounds SR144528²⁰ and JWH133.²¹

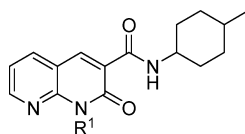
First efforts to improve the CB2R affinity and selectivity were focused on the introduction of a large variety of alkyl substituents in position N-1 of the 1,8-naphthyridine nucleus. Compounds bearing *n*-butyl (**1**) and *n*-pentyl chains (**2**) display excellent affinities for CB2R and low affinities at CB1R, so these compounds behave similarly to previously studied compounds **A1** and **A2**.

Interestingly, compounds **3**–**7**, characterized by a hydroxyalkyl chain, show no affinity toward CB1R, while their CB2R affinity increases with the elongation of the alkyl chain length. In fact, the replacement of the hydroxyethyl group of **3** with a three-carbon (hydroxypropyl in compound **4**), a four-carbon

linker (hydroxybutyl in compound **5**), or a five-carbon linker (hydroxypentyl in compound **6**) progressively increased CB2R affinity (K_i values varying from 2096 nM to 3.60 nM). On the contrary, compound **7** possessing a further elongated hydroxyhexyl chain, displays a slight loss in CB2R affinity (K_i = 18.0 nM).

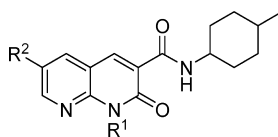
The replacement of the hydroxy group by a fluorine atom allows to increase affinity for CB2R, but significantly decreases the selectivity toward this receptor (see compounds **15**, **16**), with the exception of compound **14**, which has the highest selectivity obtained for fluoroalkyl compounds ($K_i(\text{CB1})/K_i(\text{CB2})$ = 743).

Finally, the esters **8**–**10** display a good CB2R affinity and no affinity toward CB1R (K_i > 10 000 nM), thus showing an

Table 1. Radioligand Binding Data of 1,8-Naphthyridin-2(1H)-one-3-carboxamide Derivatives 1–16^a

compd	R ¹	K _i (nM)		K _i (CB1)/K _i (CB2)
		CB1 ^b	CB2 ^c	
1	CH ₂ (CH ₂) ₂ CH ₃	2314 ± 108	3.90 ± 0.17	593
2	CH ₂ (CH ₂) ₃ CH ₃	908 ± 19.3	2.82 ± 0.08	322
3	CH ₂ CH ₂ OH	>10 000	2096 ± 98.8	>5
4	CH ₂ (CH ₂) ₂ OH	>10 000	129 ± 5.55	>77
5	CH ₂ (CH ₂) ₃ OH	>10 000	53.3 ± 1.22	>187
6	CH ₂ (CH ₂) ₄ OH	>10 000	3.60 ± 0.13	>2778
7	CH ₂ (CH ₂) ₃ OH	>10 000	18.0 ± 0.26	>554
8	CH ₂ CH ₂ COOEt	>10 000	176 ± 7.3	>57
9	CH ₂ (CH ₂) ₂ COOEt	>10 000	62.6 ± 0.79	>160
10	CH ₂ (CH ₂) ₃ COOMe	>10 000	27.1 ± 0.77	>369
11	CH ₂ CH ₂ COOH	>10 000	1394 ± 62.3	>7
12	CH ₂ (CH ₂) ₂ COOH	>10 000	2466 ± 95.5	>4
13	CH ₂ (CH ₂) ₃ COOH	>10 000	1341 ± 53.4	>7
14	CH ₂ (CH ₂) ₃ F	1011 ± 46.5	1.36 ± 0.053	743
15	CH ₂ (CH ₂) ₄ F	22.59 ± 1.02	0.56 ± 0.013	40.3
16	CH ₂ (CH ₂) ₃ F	35.67 ± 1.09	1.46 ± 0.014	24.4
A1	morpholinoethyl	1000	1.90	526
A2	<i>p</i> -fluorobenzyl	200	0.90	222
SR144528		437	0.60	728
JWH133		677	3.00	226

^aData represent mean values for at least three separate experiments performed in duplicate and are expressed as K_i (nM) for CB1R and CB2R binding assays. ^bAffinity of compounds for CB1R was evaluated using membranes from HEK-293 cells transfected with CB1R and [³H]CP-55,940. ^cAffinity of compounds for CB2R was evaluated using membranes from HEK-293 cells transfected with CB2R and [³H]CP-55,940.

Table 2. Radioligand Binding Data of 6-Substituted 1,8-Naphthyridin-2(1H)-one-3-carboxamide Derivatives 17–26^a

compd	R ¹	R ²	K _i (nM)		K _i (CB1)/K _i (CB2)
			CB1 ^b	CB2 ^c	
17	<i>p</i> -fluorobenzyl	Br	96.1 ± 1.99	0.18 ± 0.002	534
17- <i>trans</i>	<i>p</i> -fluorobenzyl	Br	166 ± 7.7	1.12 ± 0.01	148
17- <i>cis</i>	<i>p</i> -fluorobenzyl	Br	121 ± 5.32	0.12 ± 0.002	1010
18	morpholinoethyl	Br	750 ± 26.5	1.26 ± 0.04	595
19	<i>p</i> -fluorobenzyl	<i>p</i> -methoxyphenyl	3262 ± 101	3.83 ± 0.05	851
20	<i>p</i> -fluorobenzyl	2-thienyl	3280 ± 116	1.85 ± 0.06	1773
20- <i>trans</i>	<i>p</i> -fluorobenzyl	2-thienyl	430 ± 20.2	65.6 ± 2.41	6.5
20- <i>cis</i>	<i>p</i> -fluorobenzyl	2-thienyl	472 ± 20.6	0.96 ± 0.035	491
21	<i>p</i> -fluorobenzyl	<i>p</i> -fluorophenyl	>10 000	2.17 ± 0.09	>4608
22	<i>p</i> -fluorobenzyl	2-furyl	3444 ± 170.5	0.67 ± 0.009	5140
22- <i>trans</i>	<i>p</i> -fluorobenzyl	2-furyl	>10 000	94.2 ± 2.47	>106
22- <i>cis</i>	<i>p</i> -fluorobenzyl	2-furyl	4056 ± 200	0.27 ± 0.004	15 022
23	morpholinoethyl	<i>p</i> -methoxyphenyl	>10 000	1.47 ± 0.05	>6802
24	morpholinoethyl	2-thienyl	32.7 ± 1.48	0.17 ± 0.002	192
25	morpholinoethyl	<i>p</i> -fluorophenyl	66.7 ± 2.33	0.68 ± 0.009	98
26	morpholinoethyl	2-furyl	52.9 ± 1.90	0.35 ± 0.01	151

^aData represent mean values for at least three separate experiments performed in duplicate and are expressed as K_i (nM) for CB1R and CB2R binding assays. ^bAffinity of compounds for CB1R was evaluated using membranes from HEK-293 cells transfected with CB1R and [³H]CP-55,940. ^cAffinity of compounds for CB2R was evaluated using membranes from HEK-293 cells transfected with CB2R and [³H]CP-55,940.

important degree of CB2R selectivity. The corresponding carboxylic acids **11–13** show no affinity toward CB1R ($K_i > 10\,000$ nM) but also very low CB2R affinity.

Next, with the aim to investigate the impact on the CB2R affinity and selectivity within this series of 1,8-naphthyridin-2(1*H*)-one-3-carboxamides, various lipophilic groups were introduced at the position C-6 (Table 2). In details, compounds **17–26** are characterized by the presence of the common 4-methylcyclohexyl carboxamide moiety at position C-3 together with a *p*-fluorobenzyl or a morpholinoethyl group at position N-1 of the naphthyridine scaffold, since these groups had been shown to be important for CB2R affinity in our previous studies.¹⁹

All of these 6-substituted analogues (**17–26**) maintain high CB2R affinities ($K_i < 4$ nM) relative to the corresponding compounds lacking the substituent in position C-6 (**A1** and **A2**, Table 1), with the exception of compounds **20-trans** and **22-trans**.

With regard to the *N-p*-fluorobenzyl derivatives, the compounds substituted in position 6 with a bromine atom (**17**) exhibits a K_i value at CB2R (0.18 nM) slightly lower than that of its reference analogue **A2** (0.90 nM), while the selectivity for CB2R of this new compound is considerably greater (**A2**, $K_i(\text{CB2})/K_i(\text{CB1}) = 222$; **17**, $K_i(\text{CB2})/K_i(\text{CB1}) = 534$). The introduction of aromatic groups, such as *p*-methoxyphenyl (**19**), thienyl (**20**), *p*-fluorophenyl (**21**), or furyl (**22**), in position 6 of the naphthyridine nucleus generally results in a significantly reduced affinity for the CB1R, when compared to that of unsubstituted compound **A2** or 6-bromine-substituted **17**. Moreover, for some of these compounds (**17**, **20**, and **22**) the *cis* and *trans* isomers were separated in order to assess the effect of stereoselectivity on the CB2R affinity. Pure isomers **17-cis**, **20-cis**, and **22-cis** showed 9-fold, 68-fold, and 349-fold increases in their affinity for the CB2R when compared with their corresponding diastereoisomers **17-trans**, **20-trans**, and **22-trans**. These data confirm our previously hypothesis that the *cis* conformation is the preferred one for the interaction of 4-methylcyclohexyl carboxamide derivatives at CB2R.¹⁹

More surprisingly, substitution in position C-6 of morpholinoethyl derivatives (**18**, **23–26**) did not significantly alter CB2R binding affinity respect to the corresponding *N-p*-fluorobenzyl-substituted derivatives, but determined a general enhancement of the affinity on CB1R, with the exception of compound **23**, which has a K_i for CB1R higher than 10 000 nM.

CB2R Functional Activity. The potency and efficacy of the new ligands **5**, **14**, **17**, **18**, and **23** and of previously studied derivatives **A1** and **A2** were characterized with a β -arrestin 2 assay using U2OS cells co-expressing CB2R and β -arr2/GFP as previously described.²² We chose these representative compounds in order to assess the impact of the substitution in positions 1 and 6 of the naphthyridine nucleus on the functional activity. Furthermore, we have compared the pharmacology observed using the β -arrestin 2 recruitment assay for compounds **A1**, **A2**, **14**, and **18** with the effects on forskolin-stimulated cAMP levels (Perkin-Elmer LANCE) in the same cell line (Table 3).

Using the β -arrestin 2 assay, four agonists at CB2R were determined, **A1**, **A2**, **5**, and **14**, with CB2R EC_{50} values ranging from 17.6 to 29.6 nM (Figure 2, Table 3), while **17**, **18**, and **23** showed a reduction of basal β -arrestin recruitment, therefore suggesting that these compounds act as inverse agonists as well

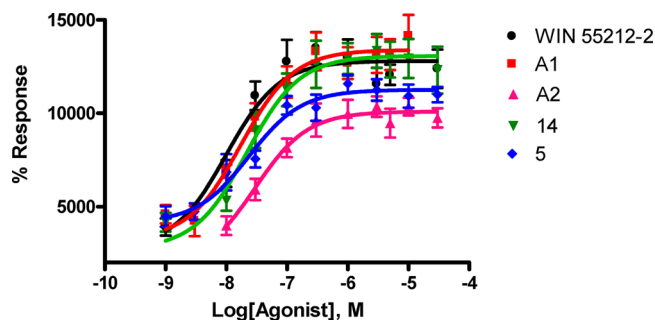


Figure 2. Concentration–response curves depicting β arr2-GFP recruitment following treatment with CB2R agonists. EC_{50} values are reported in Table 3. Activity values were normalized to the agonist's response (30 nM WIN-55,212–2 was considered as 100%). Data are the mean \pm SE of three experiments carried out in duplicate.

as antagonists (Figure 3, Table 3). The functionality of the cannabinoid agonist WIN-55,212-2 and the antagonist SR144528 were determined as reference compounds.

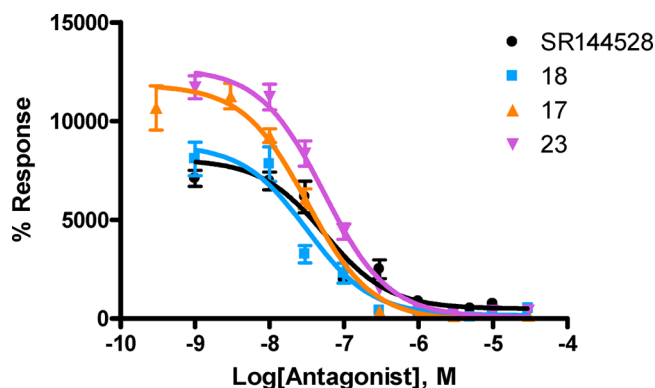


Figure 3. WIN-55,212–2 mediated β arr2-GFP recruitments is blocked by CB2R antagonists. IC_{50} values are reported in Table 3. Activity values were normalized to the agonist's response (30 nM WIN-55,212–2 was considered as 100%). Data are the mean \pm SE of three experiments carried out in duplicate.

The ability of selected compounds **A1**, **A2**, **14**, and **18** to activate CB2R was assessed in a functional cAMP assay using U2OS cells stably expressing human CB2R. Unfortunately, compounds **5**, **17**, and **23** proved to be insoluble under the test conditions. Similar to the agonist WIN-55,212-2 ($EC_{50} = 17.3$ nM), **A1**, **A2**, and **14** potently inhibited forskolin-mediated cAMP production by human CB2R, with $EC_{50} = 28.0$, 29.6, and 20.6 nM, respectively (Figure 4, Table 3). The inhibition curve of antagonist/inverse agonists **18** on human CB2R stimulated with WIN-55,212-2 (30 nM) is reported in Figure 5, and $IC_{50} = 59.6$ nM.

Table 3 shows an overall good correlation between the EC_{50} and IC_{50} values obtained using all three methodologies. With the cell-based activity data, we demonstrated an analogue functional activity for compounds **A1**, **A2**, **14**, and **18**, which indicates that both pathways, β -arrestin and GPCR, are pharmacologically modulated by these ligands. Replacement of *p*-fluorobenzyl (**A2**) and morpholinoethyl (**A1**) groups with alkyl groups, such as 4-hydroxybutyl (**5**) and 4-fluorobutyl (**14**), in position N-1 was well tolerated, maintaining agonist activity and potency in the β -arrestin and cAMP assays (compare **A1** and **A2** with **5** and **14**). Interestingly the tested

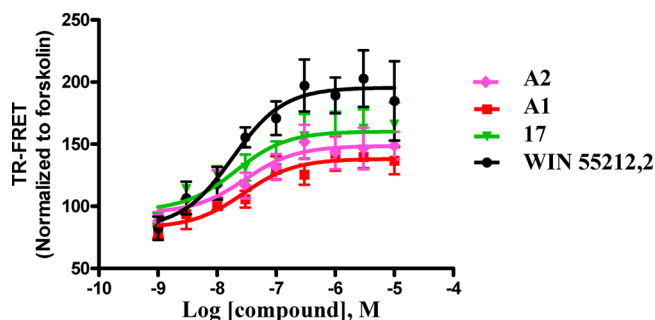


Figure 4. CB2R Agonists inhibit cAMP formation. Higher TR-FRET signals correlates with lower cAMP levels. EC_{50} Values are reported in Table 3. Data are the mean \pm SE of three experiments carried out in triplicate.

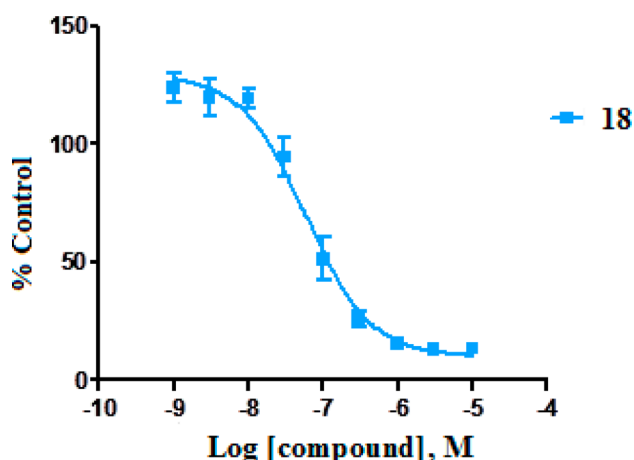


Figure 5. Treatment with the CB2R antagonist/inverse agonist **18** inhibits the response to WIN-55,212-2 in the cAMP assay. IC_{50} value is reported in Table 3. Data are the mean \pm SE of three experiments carried out in triplicate.

compounds acted as agonists or antagonists/inverse agonists in functional activity assays, depending on the presence of the substituents at position C-6 of the naphthyridine scaffold. In fact, the introduction of substituents (bromine or *p*-methoxyphenyl) in this position determined a functionality switch from agonist to antagonists/inverse agonists (see compounds **17**, **18**, and **23**).

Docking Study. The Key Molecular Features That Discriminate 1,8-Naphthyridin-2(1H)-one-3-carboxamide Derivative Agonists from Antagonists/Inverse Agonists. As we reported previously,^{19,23} the *cis* structural isomer of the 4-methylcyclohexyl substituent has higher affinity for CB2R than the *trans* structural isomer by 7–13-fold. Therefore, in the docking studies reported below, the lowest energy *cis* positional isomer was used. The conformational analysis of antagonists/inverse agonists **17**, **18**, **23**, and the agonists **A2**, **A1**, **5**, **14** is reported in Supporting Information.

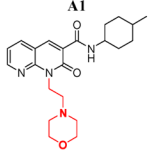
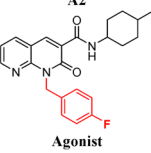
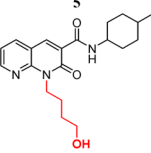
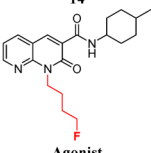
Molecular Toggle Switch. Agonist binding triggers the changes in the intracellular region of a GPCR that leads to the activated state. The CB2R TMH6 flexible hinge (CWXP) residue, W6.48(258), in the R (inactive) state, has a g^+ χ^1 dihedral angle. (Please see Experimental Section for explanation of Ballesteros–Weinstein residue nomenclature.) In the Class A GPCR, rhodopsin, the β -ionone ring of the covalently bound ligand, 11-*cis*-retinal, sterically keeps W6.48(265) in a g^+ χ^1 .^{24–26} In the X-ray crystal structure of a constitutively active

rhodopsin mutant, the transition of the ligand from 11-*cis*-retinal to *all-trans*-retinal releases W6.48(265). The β -ionone ring shifts 4.3 Å toward the cleft between TMH5 and TMH6 and the W6.48(265) indole ring moves 3.6 Å away from its ground-state position when rhodopsin is activated.²⁷ Mutation studies have suggested that F3.36(200) serves the same function in the CB1R as the β -ionone ring serves in rhodopsin.^{28,29} These residues form a “toggle switch” in which the CB1R F3.36(200) χ^1 must undergo a *trans* \rightarrow g^+ conformational change in order for the χ^1 of W6.48(356) to undergo its g^+ \rightarrow *trans* transition. In CB2R, F3.36(117) appears to serve a similar function in holding W6.48(258) in a g^+ χ^1 conformation. Agonist binding promotes a conformational change in these residues (F3.36(117) χ^1 *trans* \rightarrow g^+ ; W6.48(258) χ^1 g^+ \rightarrow *trans*). The W6.48 χ^1 has not been found in the *trans* conformation in recent X-ray crystal structures of GPCR activated states. However, in their meta-rhodopsin II crystal structure paper, Choe and co-workers note that the W6.48(265) χ^1 g^+ \rightarrow *trans* change may be transient and therefore not captured in the crystalline state.³⁰ In fact, in molecular dynamics simulations of cannabinoid CB2R activation by its endogenous ligand (2-AG), we observed such a transient change in W6.48(258).³¹ Interestingly, while the results of mutagenesis studies suggest that the toggle switch found in the cannabinoid receptors is comprised of F3.36(117) and W6.48(265), these residues do not necessarily form the toggle switch in all GPCRs. For example, Kobilka and co-workers have reported that in the β_2 adrenergic receptor, the residues F6.48(286) and F6.52(290) may form a rotamer toggle switch that changes conformation upon receptor activation.³² These results may suggest that while the identity of the participating residues may vary, the functional role of the toggle switch appears to be conserved among numerous GPCRs.

Glide Docking Studies Suggest the Difference between Inverse Agonists and Agonists May Depend on Interaction with Toggle Switch. Glide docking studies in our previously published model of the CB2R inactive and active states³¹ using the global minimum energy conformer revealed that both the antagonists/inverse agonists **17**, **18**, and **23**, and the agonists **A2**, **A1**, **5**, and **14**, bind in the TMH2-3-6-7 region of CB2R. Modeling studies suggested that the difference between the pharmacology of the CB2R ligands synthesized here (antagonist/inverse agonist vs agonist) may be in the ability/inability to block the Toggle Switch W6.48(258) (χ^1 g^+ \rightarrow *trans*) transition. Compounds **23** and **A1** form an antagonist/agonist pair of structurally related compounds. Figure 6A,B illustrates the complex of the CB2R with antagonist/inverse agonist **23**. Compound **23** binds in the TMH2-3-6-7 region of CB2R, establishing a hydrogen bond with K3.28(109) via the 1,8-naphthyridine carbonyl at C2. Compound **23** also forms a hydrogen bond with S7.39(285) via the carboxamide oxygen. The 1,8-naphthyridine ring also has a tilted-T aromatic stack with F2.57(87) and a tilted-T aromatic stack with W5.43(194). The 6 position *p*-methoxyphenyl substituent has a direct tilted-T aromatic stack with the aromatic ring of W6.48(258) and an offset parallel aromatic stack with W5.43(194).

Figure 6C,D illustrates the complex of the CB2R with the agonist **A1**. In the TMH2-3-6-7 region of CB2R, **A1** establishes a hydrogen bond with K3.28(109) via the 1,8-naphthyridine carbonyl oxygen at C2 and a hydrogen bond with S7.39(285)

Table 3. Affinities and Potencies of CB₂ Ligands Obtained from Binding, Second Messenger, and Receptor β -Arrestin Interaction Assays^a

Comps	CB2R Binding Assay (nM)		β -Arrestin (CB2R)		cAMP (CB2R)		Comps	CB2R Binding Assay (nM)		β -Arrestin (CB2R)		cAMP (CB2R)		
	K _i	IC ₅₀	EC ₅₀ /IC ₅₀ (nM)	EC ₅₀ /IC ₅₀ (nM)	K _i	IC ₅₀		EC ₅₀ /IC ₅₀ (nM)	EC ₅₀ /IC ₅₀ (nM)					
 A1 Agonist	1.90	2.89	17.6 (17.0-18.2)	28.0 (26.7-29.3)	17	0.18	0.72	31.6 (30.1-33.2)	--	18	1.26	4.95	32.1 (30.8-33.4)	59.6 (56.7-62.5)
 A2 Agonist	0.90	1.37	29.6 (28.4-30.8)	29.6 (28.1-31.1)	23	1.47	5.56	54.0 (52.1-55.9)	--	14	1.36	5.35	21.8 (22.8-20.7)	20.6 (19.8-21.3)
 5 Agonist	53.3	210	23.7 (22.8-24.6)	--	17	0.18	0.72	31.6 (30.1-33.2)	--	18	1.26	4.95	32.1 (30.8-33.4)	59.6 (56.7-62.5)
 14 Agonist	1.36	5.35	21.8 (22.8-20.7)	20.6 (19.8-21.3)	23	1.47	5.56	54.0 (52.1-55.9)	--	14	1.36	5.35	21.8 (22.8-20.7)	20.6 (19.8-21.3)

^aData represent mean values for at least three separate experiments performed in duplicate.

via the carboxamide oxygen. **A1** does not form aromatic stacking interactions with W5.43(194) or W6.48(258).

Compounds **23** and **A1** differ only in their C-6 substituent. In **23**, the C-6 substituent is a *p*-methoxyphenyl group, while at **A1**, the substituent is hydrogen. Because the 6 position points directly intracellular, it extends deep enough in the binding pocket to block the movement of W6.48(258) (χ_1 *g*⁺ \rightarrow *trans*), thus rendering **23** an antagonist/inverse agonist (see Figure 6B). In contrast, since **A1** lacks the large 6-substituent, it does not extend deep enough to influence W6.48(258), leaving this residue free to change conformation and therefore for the receptor to activate (see Figure 6D).

Similarly, the antagonists/inverse agonists **17** and **18** have large bromo substituents at the 6 position that would also block toggle switch transition (for compound **17** see Supporting Information, Figure S6), whereas agonists **A1**, **A2**, **5**, and **14** do not (see Supporting Information, discussion on ligand complexes and Figure S5).

CONCLUSION

In our study, in order to improve the CB₂R affinity and selectivity and to develop an exhaustive structure–activity relationship (SAR) for the series of 1,8-naphthyridin-2(1*H*)-one-3-carboxamides as CB₂R ligands, we synthesized and evaluated several new derivatives belonging to this chemical class. These compounds are characterized by the same central scaffold and are variously functionalized with different substituents in position N-1 or C-6. Generally, the new compounds exhibited good selectivities and remarkable affinities for the CB₂R. In particular, all the 6-substituted analogues showed high CB₂R affinity, with K_i < 4 nM.

Furthermore, the functional activity of more representative compounds was determined by the β -arrestin 2 assay using U2OS cells co-expressing CB₂R and β -arr2/GFP and the forskolin-stimulated cAMP assay. The potency values (IC₅₀ or EC₅₀) of the novel compounds measured in functional assays are in the nanomolar range and are closely correlated with the high-affinity values (expressed as K_i). An interesting observation in our SAR is the significant difference in the functional activity between the 6-substituted derivatives and the compounds lacking this substituent. In fact, the functionality of this new series of 1,8-naphthyridine was not affected by several modifications in position N-1, showing agonist behavior, while all the 6-substituted derivatives tested possess antagonist/inverse agonist properties at CB₂R.

To better understand the SAR results, we performed a docking study for the tested compounds using a CB₂R homology model. In particular, the complex of CB₂R in its inactive state (R) with antagonist and the complex of CB₂R in its activated state (R*) with agonist were analyzed. The results showed that both the antagonists/inverse agonist and the agonist bind in the TMH2-3-6-7 regions of CB₂R. The difference between the pharmacology of these ligands (antagonist/inverse agonist vs agonist) may be in the ability/inability to block the Toggle Switch W6.48(258) (χ_1 *g*⁺ \rightarrow *trans*) transition. We demonstrated that the substituent at the C-6 position of the central nucleus is crucial for the functionality, identifying it as the key molecular feature that discriminates 1,8-naphthyridin-2(1*H*)-one-3-carboxamide agonists from antagonists/inverse agonists.

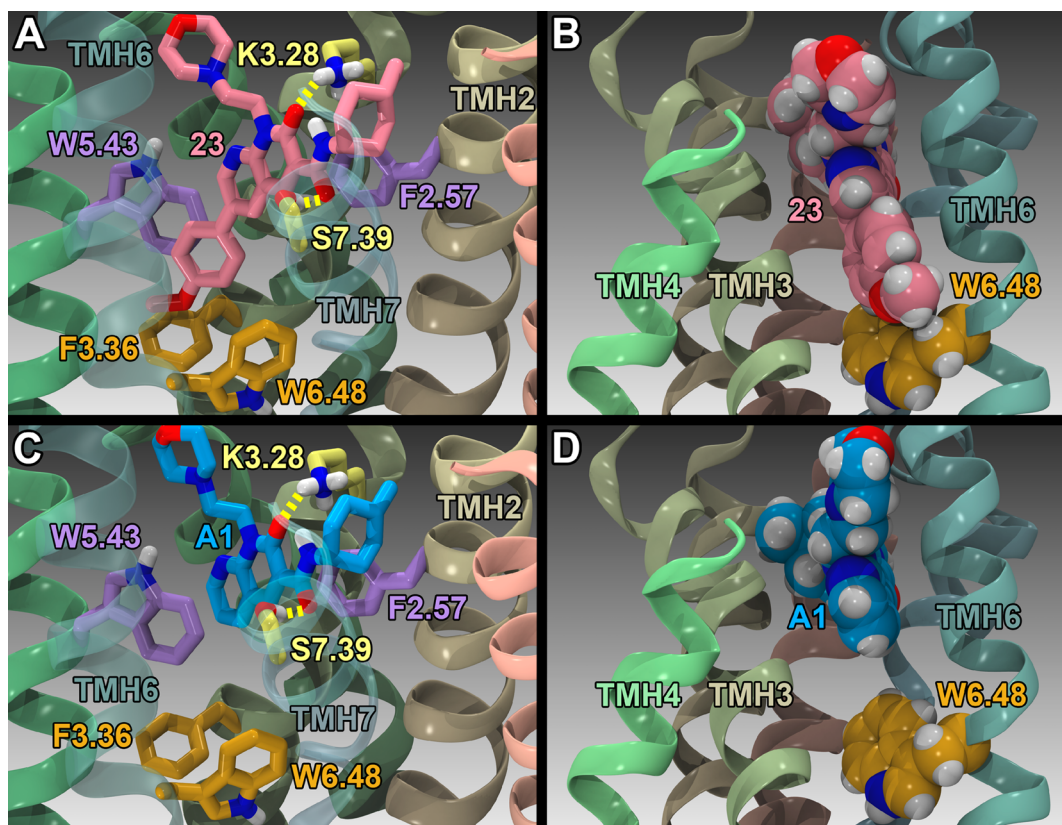


Figure 6. Binding sites and spatial relationship with W6.48(258) of the antagonist/inverse agonist **23** and the agonist **A1**, docked in CB2R (inactive) model. (A,C) The view is from lipid looking toward TMH6 and TMH7 (transparent for clarity). **23** is shown in pink; **A1** is shown in blue. Toggle switch residues are shown in orange; aromatic cluster residues are shown in lavender; residues that each ligand forms a hydrogen bond with are shown in yellow. Hydrogen bonds are shown as yellow dashed lines. (B,D) The view is from lipid looking toward TMH4 and TMH6 (TMH5 is omitted for clarity). In (B), the *p*-methoxyphenyl C6 substituent of **23** penetrates deeply into the binding pocket, deep enough to block any possible movement of W6.48(258). The ability of this substituent to block W6.48(258) likely renders **23** an antagonist/inverse agonist. In contrast, in (D) it is clear that **A1** does not penetrate the binding pocket deeply enough to sterically block W6.48(258), permitting this compound to act as an agonist.

EXPERIMENTAL SECTION

Chemistry. Melting points were determined on a Kofler hot-stage apparatus and are uncorrected. ^1H NMR and ^{13}C NMR spectra were recorded on a Varian Gemini 200 MHz spectrometer in δ units with TMS as an internal standard. Mass spectra were obtained with a Hewlett-Packard MS system 5988. TLC was performed on silica gel sheets (silica gel 60 F254, Merck, Germany). Microwave-assisted reactions were run in a CEM microwave synthesizer. The system for isocratic flash chromatography includes a Buchi Pump Module C-601 (continuous flow of solvents up to 250 mL/min at a maximum of 10 bar) and Buchi prepacked cartridges (silica gel 60, particle size 40–63 μm).

The analytical HPLC system consisted of a Thermo Finnigan Spectra System SN4000 system controller, coupled to a P2000 pump, a SCM1000 degasser, and a UV2000 UV detector at operation wavelengths of 220 and 280 nm (Thermo Finnigan, Waltham, MA). Separation was performed on a 150 mm \times 4.6 mm Luna column packed with 5 μm C18 particles. The mobile phase, delivered at isocratic flow, consisted of methanol (15–30%) and water (85–70%). HPLC-grade methanol was acquired from Sigma-Aldrich (Sydney, Australia), and the water used was of Milli-Q grade purified by a Milli-Q UV purification system (Millipore Corp., MA). For all compounds, 1.0 mg was dissolved in 2.0 mL of MeOH, and an amount of 20 μL was injected in analytical HPLC. Comparing the chromatograms, we were able to estimate the purity of each compound that appeared >96%. High-resolution mass spectra (HRMS) were recorded on a Thermo Scientific Q Exactive Plus mass spectrometer (ThermoFisher, Bremen, Germany) equipped with an electrospray ionization source.

General Procedure for the Synthesis of N-1-Substituted N-(4-methylcyclohexyl)-2-oxo-1,2-dihydro-1,8-naphthyridine-3-carboxamide (1–10). A solution of 1,8-naphthyridine-3-carboxamide **30** (1.42 g, 5.0 mmol) in anhydrous DMF (20 mL) was treated with cesium carbonate (0.43 g, 14.0 mmol) at room temperature for 1 h. The appropriate reagent (10.0 mmol) was added, and the mixture was stirred for 12 h at 50 $^\circ\text{C}$. After cooling the reaction mixture was evaporated *in vacuo*, yielding the crude products which were purified by crystallization or flash chromatography.

1-Butyl-N-(4-methylcyclohexyl)-2-oxo-1,2-dihydro-1,8-naphthyridine-3-carboxamide (1). Purified by flash chromatography (hexane/ethyl acetate 2:1). Yield 61%; MS m/z 341 (M^+). ^1H NMR (CDCl_3): δ 10.03 and 9.65 (2m, 1H, NH), 8.88 (s, 1H, Ar), 8.73 (dd, $J = 4.6$ and 1.8 Hz, 1H, Ar), 8.07 (dd, $J = 7.4$ and 2.0 Hz, 1H, Ar), 7.27 (m, 1H, Ar), 4.61 (t, $J = 7.6$ Hz, 2H, CH_2), 4.26 and 3.95 (2m, 1H, CH), 1.84–0.89 (m, 19H, cyclohexyl + CH_2 + CH_3). ^{13}C NMR (CDCl_3): δ 162.16, 162.02, 152.09, 149.66, 140.96, 138.71, 123.47, 119.23, 115.11, 49.84, 45.97, 38.54, 34.21, 33.41, 32.21, 31.38, 30.43, 30.55, 29.90, 29.71, 24.78, 22.31, 21.85, 14.20. HRMS-ESI: m/z calcd for $\text{C}_{20}\text{H}_{27}\text{N}_3\text{O}_2$ [$\text{M}+\text{H}$] $^+$, 342.2182; found 342.2171.

N-(4-Methylcyclohexyl)-2-oxo-1-pentyl-1,2-dihydro-1,8-naphthyridine-3-carboxamide (2). Yield 85%; crystallized from diisopropyl ether; MS m/z 355 (M^+). ^1H NMR (CDCl_3): δ 10.05 and 9.69 (2m, 1H, NH), 8.85 (s, 1H, Ar), 8.71 (m, 1H, Ar), 8.06 (m, 1H, Ar), 7.27 (m, 1H, Ar), 4.58 (t, $J = 7.3$ Hz, 2H, CH_2), 4.25 and 3.96 (2m, 1H, CH), 1.84–0.92 (m, 21H, cyclohexyl + CH_2 + CH_3). ^{13}C NMR (CDCl_3): δ 162.34, 162.01, 152.15, 149.80, 141.79, 138.65, 123.36, 119.15, 115.21, 49.63, 45.49, 38.93, 34.22, 33.08, 32.15, 31.87, 30.55, 30.48, 29.91, 29.66, 24.23, 23.61, 22.14, 21.38, 14.35. HRMS-ESI: m/z calcd for $\text{C}_{21}\text{H}_{29}\text{N}_3\text{O}_2$ [$\text{M}+\text{H}$] $^+$, 356.2338; found 356.2326.

1-(2-Hydroxyethyl)-N-(4-methylcyclohexyl)-2-oxo-1,2-dihydro-1,8-naphthyridine-3-carboxamide (3). Purified by flash chromatography (hexane/ethyl acetate 2:3). Yield 55%; MS m/z 329 (M^+). 1H NMR (DMSO): δ 10.00 and 9.62 (2m, 1H, NH), 8.88 (s, 1H, Ar), 8.78 (m, 1H, Ar), 8.07 (m, 1H, Ar), 7.44 (m, 1H, Ar), 4.62 (m, 2H, CH₂), 4.26 and 3.95 (2m, 1H, CH), 4.17 (exchangeable proton, 1H, OH), 3.67 (m, 2H, CH₂), 1.84–0.89 (m, 12H, cyclohexyl + CH₃). ^{13}C NMR (CDCl₃): δ 162.45, 162.07, 152.25, 149.34, 141.89, 138.64, 123.23, 119.21, 115.22, 61.71, 49.55, 45.41, 41.72, 34.45, 33.72, 32.42, 31.73, 30.42, 29.96, 22.15, 21.38. HRMS-ESI: m/z calcd for C₁₈H₂₃N₃O₃ [$M+H$]⁺, 330.1818; found 330.1807.

1-(3-Hydroxypropyl)-N-(4-methylcyclohexyl)-2-oxo-1,2-dihydro-1,8-naphthyridine-3-carboxamide (4). Purified by flash chromatography (hexane/ethyl acetate 1:1.5). Yield 51%; MS m/z 343 (M^+). 1H NMR (DMSO): δ 10.00 and 9.62 (2m, 1H, NH), 8.88 (s, 1H, Ar), 8.78 (m, 1H, Ar), 8.07 (m, 1H, Ar), 7.44 (m, 1H, Ar), 4.55 (m, 2H, CH₂), 4.26 and 3.95 (2m, 1H, CH), 4.19 (exchangeable proton, 1H, OH), 3.52 (m, 2H, CH₂), 1.84–0.89 (m, 14H, cyclohexyl + CH₂ + CH₃). ^{13}C NMR (CDCl₃): δ 162.71, 162.12, 152.11, 149.34, 141.65, 138.64, 123.23, 119.21, 115.12, 62.07, 49.00, 45.91, 41.46, 34.15, 33.28, 32.12, 31.30, 30.63, 30.54, 29.44, 22.14, 21.26. HRMS-ESI: m/z calcd for C₁₉H₂₅N₃O₃ [$M+H$]⁺, 344.1974; found 344.1963.

1-(4-Hydroxybutyl)-N-(4-methylcyclohexyl)-2-oxo-1,2-dihydro-1,8-naphthyridine-3-carboxamide (5). Purified by flash chromatography (hexane/ethyl acetate 1:2). Yield 63%; MS m/z 357 (M^+). 1H NMR (DMSO): δ 10.01 and 9.61 (2m, 1H, NH), 8.81 (s, 1H, Ar), 8.66 (dd, J = 4.4 and 1.7 Hz, 1H, Ar), 8.04 (dd, J = 7.2 and 2.0 Hz, 1H, Ar), 7.24 (m, 1H, Ar), 4.55 (m, 2H, CH₂), 4.28 and 3.89 (2m, 1H, CH), 4.18 (exchangeable proton, 1H, OH), 3.73 (m, 2H, CH₂), 1.84–0.89 (m, 16H, cyclohexyl + CH₂ + CH₃). ^{13}C NMR (CDCl₃): δ 162.54, 162.12, 151.97, 149.64, 141.87, 138.81, 123.09, 119.27, 115.12, 62.56, 49.12, 45.79, 41.14, 34.33, 33.51, 32.12, 31.11, 30.44, 29.43, 29.86, 25.75, 22.37, 21.22. HRMS-ESI: m/z calcd for C₂₀H₂₇N₃O₃ [$M+H$]⁺, 358.2131; found 358.2120.

1-(5-Hydroxypentyl)-N-(4-methylcyclohexyl)-2-oxo-1,2-dihydro-1,8-naphthyridine-3-carboxamide (6). Purified by flash chromatography (hexane/ethyl acetate 1:2). Yield 85%; MS m/z 371 (M^+). 1H NMR (CDCl₃): δ 10.03 and 9.64 (2m, 1H, NH); 8.87 (s, 1H, Ar); 8.72 (m, 1H, Ar); 8.08 (m, 1H, Ar); 7.28 (m, 1H, Ar); 4.61 (m, 2H, CH₂); 4.27 and 3.89 (2m, 1H, CH); 4.15 (exchangeable proton, 1H, OH) 3.69 (m, 2H, CH₂); 1.82–0.92 (m, 18H, cyclohexyl + CH₂ + CH₃). ^{13}C NMR (CDCl₃): δ 162.21, 162.04, 152.2, 149.58, 142.06, 138.34, 123.05, 119.37, 115.22, 62.68, 49.35, 45.92, 40.89, 34.21, 33.12, 32.33, 31.13, 30.46, 29.92, 29.78, 27.79, 25.20, 22.26, 21.35. HRMS-ESI: m/z calcd for C₂₁H₂₉N₃O₃ [$M+H$]⁺, 372.2287; found 372.2275.

1-(6-Hydroxyhexyl)-N-(4-methylcyclohexyl)-2-oxo-1,2-dihydro-1,8-naphthyridine-3-carboxamide (7). Purified by flash chromatography (hexane/ethyl acetate 1:2). Yield 71%; MS m/z 385 (M^+). 1H NMR (CDCl₃): δ 10.00 and 9.65 (2m, 1H, NH), 8.89 (s, 1H, Ar), 8.74 (m, 1H, Ar), 8.09 (m, 1H, Ar), 7.29 (m, 1H, Ar), 4.62 (m, 2H, CH₂), 4.26 and 3.89 (2m, 1H, CH), 4.16 (exchangeable proton, 1H, OH), 3.69 (m, 2H, CH₂), 1.83–0.96 (m, 20H, cyclohexyl + CH₂ + CH₃). ^{13}C NMR (CDCl₃): δ 162.32, 162.25, 152.00, 149.65, 141.48, 138.50, 123.44, 119.21, 115.10, 62.72, 49.40, 45.92, 40.90, 34.19, 33.12, 32.33, 31.43, 30.47, 29.95, 29.79, 27.68, 27.61, 25.49, 22.35, 21.48. HRMS-ESI: m/z calcd for C₂₂H₃₁N₃O₃ [$M+H$]⁺, 386.2444; found 386.2430.

Ethyl 3-(3-(4-Methylcyclohexylcarbamoyl)-2-oxo-1,8-naphthyridin-1(2H)-yl)propanoate (8). Purified by flash chromatography (toluene/ethyl acetate 1:2). Yield 33%; MS m/z 385 (M^+). 1H NMR (CDCl₃): δ 10.01 and 9.62 (2m, 1H, NH); 8.90 (s, 1H, Ar); 8.71 (dd, J = 4.6 and 1.8 Hz, 1H, Ar); 8.08 (dd, J = 7.4 and 2.0 Hz, 1H, Ar); 7.27 (m, 1H, Ar); 4.90 (m, 2H, CH₂); 4.14 (m, 2H, CH₂); 4.25 and 3.97 (2m, 1H, CH); 2.80 (m, 2H, CH₂); 1.84–0.89 (m, 15H, cyclohexyl + CH₃). ^{13}C NMR (CDCl₃): δ 173.69, 162.34, 162.18, 152.28, 149.54, 141.78, 138.58, 123.37, 119.29, 115.39, 61.47, 49.37, 45.79, 40.95, 34.26, 33.36, 33.19, 32.52, 31.43, 30.85, 30.45, 29.78, 22.23, 21.16, 15.67. HRMS-ESI: m/z calcd for C₂₁H₂₇N₃O₄ [$M+H$]⁺, 386.2080; found 386.2066.

Ethyl 4-(3-(4-Methylcyclohexylcarbamoyl)-2-oxo-1,8-naphthyridin-1(2H)-yl)butanoate (9). Purified by flash chromatography (hexane/ethyl acetate 1:1). Yield 28%; MS m/z 399 (M^+). 1H NMR (CDCl₃): δ 10.04 and 9.67 (2m, 1H, NH); 8.89 (s, 1H, Ar); 8.70 (dd, J = 4.6 and 1.8 Hz, 1H, Ar); 8.10 (dd, J = 7.4 and 2.0 Hz, 1H, Ar); 7.26 (m, 1H, Ar); 4.69 (m, 2H, CH₂); 4.15 (m, 2H, CH₂); 4.28 and 3.95 (2m, 1H, CH); 2.45 (m, 2H, CH₂); 2.15 (m, 2H, CH₂); 1.84–0.89 (m, 15H, cyclohexyl + CH₃). ^{13}C NMR (CDCl₃): δ 173.59, 162.34, 162.21, 152.34, 149.56, 142.09, 138.77, 123.41, 119.21, 115.31, 61.43, 49.88, 45.82, 40.89, 34.22, 33.31, 32.42, 31.37, 31.43, 30.44, 29.87, 23.35, 22.13, 21.46, 15.63. HRMS-ESI: m/z calcd for C₂₂H₂₉N₃O₄ [$M+H$]⁺, 400.2236; found 400.2224.

Methyl 5-(3-(4-Methylcyclohexylcarbamoyl)-2-oxo-1,8-naphthyridin-1(2H)-yl)pentanoate (10). Purified by flash chromatography (hexane/ethyl acetate 1:2). Yield 23%; MS m/z 399 (M^+). 1H NMR (CDCl₃): δ 10.03 and 9.66 (2m, 1H, NH); 8.88 (s, 1H, Ar); 8.71 (dd, J = 4.6 and 1.8 Hz, 1H, Ar); 8.09 (dd, J = 7.4 and 2.0 Hz, 1H, Ar); 7.27 (m, 1H, Ar); 4.63 (m, 2H, CH₂); 4.28 and 3.95 (2m, 1H, CH); 3.68 (1s, 3H, CH₃); 2.45 (m, 2H, CH₂); 1.82–0.83 (m, 16H, cyclohexyl + CH₂ + CH₃). ^{13}C NMR (CDCl₃): δ 173.61, 162.42, 162.23, 152.55, 149.36, 141.39, 138.87, 123.24, 119.21, 115.34, 55.82, 49.97, 45.69, 40.39, 34.27, 33.28, 33.19, 32.12, 31.43, 30.95, 30.47, 29.86, 27.41, 23.35, 22.31, 21.46. HRMS-ESI: m/z calcd for C₂₂H₂₉N₃O₄ [$M+H$]⁺, 400.2236; found 400.2223.

General Procedure for the Synthesis of the Acids 11–13. A mixture of 0.21 mmol of ester derivatives 8–10 in 15.0 mL of NaOH 10% was heated at 110 °C for 5 h. After cooling, the reaction mixture was treated with water and then with concentrated HCl until pH 2–3. The precipitate formed was filtered and treated with Et₂O to give the acid derivatives 11–13.

3-(3-(4-Methylcyclohexylcarbamoyl)-2-oxo-1,8-naphthyridin-1(2H)-yl)propanoic Acid (11). Yield 96%; MS m/z 357 (M^+). 1H NMR (DMSO): δ 12.55 (s, 1H, OH); 9.83 and 9.68 (2m, 1H, NH); 8.86 (s, 1H, Ar); 8.76 (m, 1H, Ar); 8.48 (m, 1H, Ar); 7.42 (m, 1H, Ar); 4.68 (m, 2H, CH₂); 4.25 and 3.97 (2m, 1H, CH); 2.90 (m, 2H, CH₂); 1.86–0.90 (m, 12H, cyclohexyl + CH₃). ^{13}C NMR (DMSO): δ 177.83, 161.48, 161.22, 150.42, 148.45, 142.11, 138.20, 122.44, 117.23, 113.13, 47.68, 44.97, 41.74, 37.80, 34.12, 33.31, 32.42, 31.63, 29.76, 29.25, 22.31, 21.36. HRMS-ESI: m/z calcd for C₁₉H₂₃N₃O₄ [$M+H$]⁺, 358.1767; found 358.1756.

4-(3-(4-Methylcyclohexylcarbamoyl)-2-oxo-1,8-naphthyridin-1(2H)-yl)butanoic Acid (12). Yield 92%; MS m/z 371 (M^+). 1H NMR (DMSO): δ 12.06 (s, 1H, OH); 9.96 and 9.68 (2m, 1H, NH); 8.90 (s, 1H, Ar); 8.78 (m, 1H, Ar); 8.48 (m, 1H, Ar); 7.44 (m, 1H, Ar); 4.54 (m, 2H, CH₂); 4.24 and 3.95 (2m, 1H, CH); 2.49 (m, 2H, CH₂); 1.94–0.92 (m, 14H, cyclohexyl + CH₂ + CH₃). ^{13}C NMR (DMSO): δ 177.88, 161.53, 161.36, 150.46, 148.55, 142.21, 138.22, 122.24, 117.28, 113.16, 47.72, 44.95, 43.12, 36.92, 34.15, 33.12, 32.34, 31.33, 29.65, 29.19, 23.79, 22.32, 21.34. HRMS-ESI: m/z calcd for C₂₀H₂₅N₃O₄ [$M+H$]⁺, 372.1923; found 372.1912.

5-(3-(4-Methylcyclohexylcarbamoyl)-2-oxo-1,8-naphthyridin-1(2H)-yl)pentanoic Acid (13). Yield 95%; MS m/z 385 (M^+). 1H NMR (DMSO): δ 12.05 (s, 1H, OH); 9.94 and 9.58 (2m, 1H, NH); 8.90 (s, 1H, Ar); 8.80 (dd, J = 4.6 and 1.8 Hz, 1H, Ar); 8.49 (dd, J = 7.4 and 2.0 Hz, 1H, Ar); 7.45 (m, 1H, Ar); 4.49 (m, 2H, CH₂); 4.12 and 3.85 (2m, 1H, CH); 2.29 (m, 2H, CH₂); 1.97–0.88 (m, 16H, cyclohexyl + 2CH₂ + CH₃). ^{13}C NMR (DMSO): δ 177.89, 161.42, 161.21, 150.40, 148.68, 142.00, 138.00, 122.43, 117.23, 113.19, 47.68, 44.97, 41.74, 37.82, 34.35, 33.21, 32.20, 31.33, 29.89, 29.43, 27.85, 24.09, 22.31, 21.46. HRMS-ESI: m/z calcd for C₂₁H₂₇N₃O₄ [$M+H$]⁺, 386.2080; found 386.2068.

General Procedure for the Synthesis of Mesylates 28–30. Triethylamine (0.82 mL, 0.526 g, 5.89 mmol) was added at 0 °C to a solution of suitable alcohol 5–7 (0.98 mmol) and methanesulfonyl chloride (0.23 mL, 0.34 g, 2.94 mmol) in anhydrous dichloromethane (8.0 mL), and the mixture was stirred for 6 h at ambient temperature. After addition of ethyl acetate (30 mL), the mixture was washed with water (20.0 mL) and then with brine (20.0 mL). The organic layer was dried over MgSO₄ and evaporated to dryness to give a residue which was purified by flash column chromatography.

4-(3-(4-Methylcyclohexylcarbamoyl)-2-oxo-1,8-naphthyridin-1(2H)-yl)butyl Methanesulfonate (**28**). Purified by flash chromatography (hexane/ethyl acetate 1:1). Yield 86%; MS m/z 435 (M^+). 1H NMR ($CDCl_3$): δ 9.98 and 9.63 (2m, 1H, NH); 8.83 (s, 1H, Ar); 8.67 (m, 1H, Ar); 8.08 (m, 1H, Ar); 7.26 (m, 1H, Ar); 4.61 (m, 2H, CH_2); 4.30 (m, 2H, CH_2); 4.28 and 3.89 (2m, 1H, CH); 3.01 (s, 3H, CH_3); 1.88–0.87 (m, 16H, cyclohexyl + CH_2 + CH_3). ^{13}C NMR ($CDCl_3$): δ 162.73, 161.96, 152.22, 149.78, 142.00, 138.69, 123.34, 119.35, 115.11, 69.94, 49.03, 45.83, 41.21, 37.60, 34.14, 33.21, 32.25, 31.36, 30.45, 29.88, 26.84, 24.29, 22.50, 21.87.

5-(3-(4-Methylcyclohexylcarbamoyl)-2-oxo-1,8-naphthyridin-1(2H)-yl)pentyl Methanesulfonate (**29**). Purified by flash chromatography (hexane/ethyl acetate 1:1). Yield 43%; MS m/z 449 (M^+). 1H NMR ($CDCl_3$): δ 9.99 and 9.61 (2m, 1H, NH); 8.86 (s, 1H, Ar); 8.70 (m, 1H, Ar); 8.07 (m, 1H, Ar); 7.26 (m, 1H, Ar); 4.57 (m, 2H, CH_2); 4.29 (m, 2H, CH_2); 4.18 and 3.89 (2m, 1H, CH); 3.00 (s, 3H, CH_3); 1.97–0.89 (m, 18H, cyclohexyl + CH_2 + CH_3). ^{13}C NMR ($CDCl_3$): δ 162.73, 162.05, 152.20, 149.78, 142.00, 138.62, 123.41, 119.24, 115.13, 70.05, 49.05, 45.90, 41.71, 37.64, 34.18, 33.25, 32.27, 31.32, 30.48, 29.86, 29.04, 27.44, 23.29, 22.51, 21.79.

6-(3-(4-Methylcyclohexylcarbamoyl)-2-oxo-1,8-naphthyridin-1(2H)-yl)hexyl Methanesulfonate (**30**). Purified by flash chromatography (hexane/ethyl acetate 1:1). Yield 37%; MS m/z 463 (M^+). 1H NMR ($CDCl_3$): δ 9.96 and 9.63 (2m, 1H, NH); 8.82 (s, 1H, Ar); 8.65 (m, 1H, Ar); 8.01 (m, 1H, Ar); 7.20 (m, 1H, Ar); 4.50 (m, 2H, CH_2); 4.28 (m, 2H, CH_2); 4.17 and 3.89 (2m, 1H, CH); 2.96 (s, 3H, CH_3); 1.99–0.76 (m, 20H, cyclohexyl + CH_2 + CH_3). ^{13}C NMR ($CDCl_3$): δ 162.65, 162.07, 152.13, 149.82, 141.80, 138.53, 123.41, 119.12, 115.09, 70.21, 49.02, 45.92, 41.88, 37.64, 34.18, 33.21, 32.49, 31.25, 30.45, 29.81, 29.29, 27.84, 26.68, 25.42, 22.49, 21.72.

General Procedure for the Preparation of Fluorine Derivatives 14–16. To a solution of suitable mesylate **28–30** (0.6 mmol) in anhydrous THF (10 mL) was added tetrabutylammonium fluoride (1.00 N) in THF (0.35 mL, 0.314 g, 1.2 mmol), and the mixture was refluxed for 4 h. After cooling, the solvent was removed under vacuum, and the residue was solubilized in chloroform (10 mL), washed with water (20 mL), and then washed with brine (20 mL). The organic layer was dried over $MgSO_4$ and evaporated to dryness to give crude product which was purified by flash column chromatography.

1-(4-Fluorobutyl)-1,2-dihydro-*N*-(4-methylcyclohexyl)-2-oxo-1,8-naphthyridine-3-carboxamide (**14**). Purified by flash chromatography (hexane/ethyl acetate 1.5:1). Yield 56%; MS m/z 359 (M^+). 1H NMR ($CDCl_3$): δ 10.01 and 9.62 (2m, 1H, NH); 8.88 (s, 1H, Ar); 8.71 (m, 1H, Ar); 8.08 (m, 1H, Ar); 7.28 (m, 1H, Ar); 4.66 (m, 2H, CH_2); 4.42 (m, 2H, CH_2); 4.26 and 3.93 (2m, 1H, CH); 1.92–0.91 (m, 16H, cyclohexyl + CH_2 + CH_3). ^{13}C NMR ($CDCl_3$): δ 162.76, 162.06, 152.15, 149.91, 141.89, 138.59, 123.47, 119.19, 115.13, 85.61, 82.33, 49.07, 45.94, 41.59, 34.20, 33.27, 32.29, 31.34, 30.48, 29.88, 28.44, 24.23, 22.52, 21.78. HRMS-ESI: m/z calcd for $C_{20}H_{26}FN_3O_2$ [$M+H$] $^+$, 360.2087; found 360.2076.

1-(5-Fluoropentyl)-*N*-(4-methylcyclohexyl)-2-oxo-1,2-dihydro-1,8-naphthyridine-3-carboxamide (**15**). Purified by flash chromatography (hexane/ethyl acetate 1:1). Yield 49%; MS m/z 373 (M^+). 1H NMR ($CDCl_3$): δ 10.03 and 9.64 (2m, 1H, NH); 8.88 (s, 1H, Ar); 8.71 (m, 1H, Ar); 8.09 (m, 1H, Ar); 7.26 (m, 1H, Ar); 4.59 (m, 2H, CH_2); 4.37 (m, 2H, CH_2); 4.28 and 3.95 (2m, 1H, CH); 1.82–0.92 (m, 18H, cyclohexyl + CH_2 + CH_3). ^{13}C NMR ($CDCl_3$): δ 162.77, 162.11, 152.15, 149.95, 141.84, 138.59, 123.42, 119.17, 115.15, 85.82, 82.55, 49.73, 45.96, 41.92, 34.21, 33.27, 32.30, 31.24, 30.62, 30.44, 29.88, 27.76, 24.23, 22.72, 21.76. HRMS-ESI: m/z calcd for $C_{21}H_{28}FN_3O_2$ [$M+H$] $^+$, 374.2244; found 374.2232.

1-(6-Fluorohexyl)-*N*-(4-methylcyclohexyl)-2-oxo-1,2-dihydro-1,8-naphthyridine-3-carboxamide (**16**). Purified by flash chromatography (hexane/ethyl acetate 1:1). Yield 47%; MS m/z 387 (M^+). 1H NMR ($CDCl_3$): δ 10.03 and 9.65 (2m, 1H, NH); 8.87 (s, 1H, Ar); 8.71 (m, 1H, Ar); 8.08 (m, 1H, Ar); 7.28 (m, 1H, Ar); 4.59 (m, 2H, CH_2); 4.34 (m, 2H, CH_2); 4.27 and 3.93 (2m, 1H, CH); 1.81–0.91 (m, 20H, cyclohexyl + CH_2 + CH_3). ^{13}C NMR ($CDCl_3$): δ 162.77, 162.15, 152.15, 149.95, 141.90, 138.55, 123.42, 119.10, 115.11, 85.93, 82.65, 49.05, 45.968 42.02, 34.21, 33.27, 32.30, 31.24, 30.78, 30.48,

29.90, 28.06, 26.97, 25.26, 22.72, 21.76. HRMS-ESI: m/z calcd for $C_{22}H_{30}FN_3O_2$ [$M+H$] $^+$, 388.2400; found 388.2387.

2-Amino-5-bromonicotinaldehyde (**31**). To a stirred solution of 2-aminopyridine-3-carboxaldehyde (0.40 g, 3.30 mmol) in 15 mL of glacial acetic acid was added bromine (0.16 mL, 3.16 mmol), and the reaction mixture was stirred at room temperature for 24 h. The precipitate obtained was filtered off and washed with ether. The filter cake was poured into water and treated with solid NaOH until pH 7–8, and the mixture was extracted with dichloromethane. The organic layer was dried with $MgSO_4$ and evaporated to dryness under reduced pressure. The crude solid was purified by crystallization in acetonitrile to give **31** (0.48 g, 73%); mp 147–150 °C; MS m/z 199 (M^+). 1H NMR (DMSO): δ 9.83 (s, 1H, CHO), 8.33 (s, 1H, Ar); 8.27 (s, 1H, Ar); 5.27 (br, 2H, NH_2).

Ethyl 6-Bromo-2-oxo-1,2-dihydro-1,8-naphthyridine-3-carboxylate (**32**). To a solution of **31** (1.50 g, 7.5 mmol) in ethanol (20 mL) were added diethyl malonate (1.80 g, 11.25 mmol) and 0.21 mL of piperidine (0.182 g, 2.14 mmol), and the mixture was stirred under reflux for 20 h. After cooling, the solid obtained was filtered, washed with ethanol, and dried. The crude product was used without further purifications (1.99 g, 90%); mp 200–203 °C; MS m/z 296 (M^+). 1H NMR (DMSO): δ 12.64 (br, 1H, NH); 8.69 (d, J = 2.2 Hz, 1H, Ar); 8.56 (d, J = 2.2 Hz, 1H, Ar); 8.45 (s, 1H, Ar); 4.28 (q, J = 7.3 Hz, 2H, CH_2); 1.31 (t, J = 7.1 Hz, 3H, CH_3).

6-Bromo-*N*-(4-methylcyclohexyl)-2-oxo-1,2-dihydro-1,8-naphthyridine-3-carboxamide (**33**). A mixture of **4** (0.40 g, 1.35 mmol) and 4-methylcyclohexylamine (0.76 g, 6.75 mmol) was heated in a sealed tube at 150 °C for 24 h. After cooling, the reaction mixture was treated with diethyl ether to give a solid residue which was collected by filtration. The product was crystallized from ethyl acetate (0.32 g, 65%); MS m/z 363 (M^+). 1H NMR (DMSO): δ 12.09 (br, 1H, NH); 10.06 and 9.57 (2m, 1H, NH); 8.73–8.83 (m, 3H, Ar); 4.12 and 3.78 (2m, 1H, CH); 1.90–0.89 (m, 12H, cyclohexyl + CH_3).

General Procedure for the Synthesis of 6-Bromo Derivatives 17 and 18. A solution of 6-bromo-*N*-(4-methylcyclohexyl)-2-oxo-1,2-dihydro-1,8-naphthyridine-3-carboxamide **33** (1.42 g, 5.0 mmol) in anhydrous DMF (20 mL) was treated with cesium carbonate (0.43 g, 14.0 mmol) at room temperature for 1 h. The suitable chloride (10 mmol) was added, and the mixture was stirred for 12 h at 50 °C. After cooling, the reaction mixture was evaporated *in vacuo*, yielding the crude products which were purified by flash chromatography.

6-Bromo-1-(4-fluorobenzyl)-*N*-(4-methylcyclohexyl)-2-oxo-1,2-dihydro-1,8-naphthyridine-3-carboxamide (**17**). Purified by flash chromatography (toluene/ethyl acetate 14:1 and 1% of acetic acid). Yield 71%. 1H NMR ($CDCl_3$): δ 9.92 and 9.52 (2m, 1H, NH); 8.75 (m, 2H, Ar); 8.20 (s, 1H, Ar); 7.52 (m, 2H, Ar); 7.03 (m, 2H, Ar); 5.73 (s, 2H, CH_2), 4.26 and 3.95 (2m, 1H, CH); 1.80–0.91 (m, 12H, cyclohexyl + CH_3). ^{13}C NMR ($CDCl_3$): δ 164.39, 162.75, 161.82, 152.57, 151.49, 142.35, 140.92, 138.96, 129.12, 124.75, 116.33, 115.28, 114.16, 49.47, 46.16, 44.88, 34.21, 33.25, 32.20, 31.28, 30.54, 29.86, 22.56, 21.80. HRMS-ESI: m/z calcd for $C_{23}H_{23}BrFN_3O_2$ [$M+H$] $^+$, 472.1036; found 472.1027.

trans-6-Bromo-1-(4-fluorobenzyl)-*N*-(4-methylcyclohexyl)-2-oxo-1,2-dihydro-1,8-naphthyridine-3-carboxamide (**17-trans**) and *cis*-6-Bromo-1-(4-fluorobenzyl)-*N*-(4-methylcyclohexyl)-2-oxo-1,2-dihydro-1,8-naphthyridine-3-carboxamide (**17-cis**). Compounds **17-trans** and **17-cis** were obtained from derivative **17** by flash chromatography on a silica gel (toluene/ethyl acetate 14:1 and 1% of acetic acid).

17-trans. Yield 17%; MS 471 m/z (M^+); mp 163–165 °C. 1H NMR ($CDCl_3$): δ 9.52 (m, 1H, NH); 8.75 (m, 2H, Ar); 8.20 (s, 1H, Ar); 7.45 (m, 2H, Ar); 7.02 (m, 2H, Ar); 5.72 (s, 2H, CH_2), 3.95 (m, 1H, CH); 1.79–0.91 (m, 12H, cyclohexyl + CH_3). ^{13}C NMR ($CDCl_3$): δ 164.39, 162.75, 161.82, 152.57, 151.49, 142.35, 140.92, 138.96, 129.12, 124.75, 116.33, 115.28, 114.16, 46.16, 44.88, 33.25, 31.28, 29.86, 21.80.

17-cis. Yield 8%; MS 471 m/z (M^+); mp 158–160 °C. 1H NMR ($CDCl_3$): δ 9.92 (m, 1H, NH); 8.75 (m, 2H, Ar); 8.20 (s, 1H, Ar); 7.45 (m, 2H, Ar); 7.02 (m, 2H, Ar); 5.72 (s, 2H, CH_2), 4.26 (m, 1H, CH); 1.79–0.93 (m, 12H, cyclohexyl + CH_3). ^{13}C NMR ($CDCl_3$): δ

164.39, 162.75, 161.82, 152.57, 151.49, 142.35, 140.92, 138.96, 129.12, 124.75, 116.33, 115.28, 114.16, 49.47, 44.88, 34.21, 32.20, 30.54, 22.56.

6-Bromo-N-(4-methylcyclohexyl)-1-(2-morpholinoethyl)-2-oxo-1,2-dihydro-1,8-naphthyridine-3-carboxamide (18). Yield 92% (crystallized by acetonitrile); MS 476 m/z (M^+). 1H NMR ($CDCl_3$): δ 9.97 and 9.57 (2m, 1H, NH); 8.75 (m, 2H, Ar); 8.19 (s, 1H, Ar); 4.73 (t, $J = 6.8$ Hz, 2H, CH_2), 4.24 and 3.96 (2m, 1H, CH); 3.51 (m, 4H, morpholine), 2.57 (m, 6H, morpholine + CH_2); 1.87–0.95 (m, 12H, cyclohexyl + CH_3). ^{13}C NMR ($CDCl_3$): δ 162.45, 161.52, 152.43, 148.38, 141.11, 139.93, 124.45, 116.31, 114.26, 67.24, 56.12, 54.12, 49.13, 45.89, 39.30, 34.16, 33.21, 32.25, 31.34, 30.41, 29.90, 22.52, 21.91. HRMS-ESI: m/z calcd for $C_{22}H_{29}BrN_4O_3$ [$M+H$] $^+$, 477.1501; found 477.1491.

General Procedure for the Synthesis of 6-Substituted Derivatives 19–26. A mixture of 50 mg of Ph_3P (0.20 mmol) and 10 mg of $Pd(OAc)_2$ (0.04 mmol) in dioxane (1.0 mL) was stirred under N_2 for 10 min. Then the appropriate 6-bromo derivative 17 or 18 (0.41 mmol) in 1 mL of MeOH, 0.85 mL of Na_2CO_3 (10%), and suitable boronic acid (0.82 mmol) were added. The mixture was heated by microwave radiation (CEM) at 150 °C for 10 min (power 200 W, pressure 100 psi, stirring on). The reaction mixture was then cooled to room temperature, treated with water, and extracted with dichloromethane. The combined organic layers were washed with brine, dried over anhydrous sodium sulfate, and evaporated to dryness to obtain a residue which was purified by flash chromatography on silica gel.

1-(4-Fluorobenzyl)-6-(4-methoxyphenyl)-N-(4-methylcyclohexyl)-2-oxo-1,2-dihydro-1,8-naphthyridine-3-carboxamide (19). Purified by flash chromatography (hexane/ethyl acetate 2:1). Yield 41%; MS m/z 499 (M^+). 1H NMR (DMSO): δ 10.02 and 9.61 (2m, 1H, NH); 8.92 (m, 2H, Ar); 8.18 (s, 1H, Ar); 7.55 (m, 4H, Ar); 7.05 (m, 4H, Ar); 5.82 (s, 2H, CH_2), 3.95 and 4.26 (2m, 1H, CH); 3.88 (s, 3H, CH_3); 1.60–0.92 (m, 12H, cyclohexyl + CH_3). ^{13}C NMR ($CDCl_3$): δ 164.39, 162.75, 162.12, 161.09, 150.99, 142.35, 140.87, 134.66, 133.80, 129.12, 128.89, 128.13, 125.76, 124.75, 116.33, 115.28, 115.07, 55.78, 49.47, 46.16, 44.88, 34.21, 33.25, 32.20, 31.28, 30.54, 29.86, 22.56, 21.80. HRMS-ESI: m/z calcd for $C_{30}H_{30}FN_3O_3$ [$M+H$] $^+$, 500.2349; found 500.2337.

1-(4-Fluorobenzyl)-N-(4-methylcyclohexyl)-2-oxo-6-(thiophen-2-yl)-1,2-dihydro-1,8-naphthyridine-3-carboxamide (20). Purified by flash chromatography (toluene/ethyl acetate 8:1). Yield 68%. 1H NMR ($CDCl_3$): δ 9.98 and 9.47 (2m, 1H, NH); 8.95 (m, 2H, Ar); 8.21 (s, 1H, Ar); 7.51 (m, 3H, Ar); 7.19 (m, 2H, Ar); 6.99 (m, 2H, Ar); 5.80 (s, 2H, CH_2), 4.26 and 3.94 (2m, 1H, CH); 1.82–0.95 (m, 12H, cyclohexyl + CH_3). ^{13}C NMR ($CDCl_3$): δ 164.39, 162.75, 162.12, 150.90, 142.47, 140.56, 138.85, 134.66, 133.26, 128.86, 127.92, 127.63, 125.56, 124.55, 122.8, 116.33, 115.28, 109.35, 107.89, 49.40, 44.88, 34.21, 33.25, 32.20, 31.28, 30.54, 29.86, 22.56, 21.80. HRMS-ESI: m/z calcd for $C_{27}H_{26}FN_3O_3S$ [$M+H$] $^+$, 476.1808; found 476.1797.

trans-1-(4-Fluorobenzyl)-N-(4-methylcyclohexyl)-2-oxo-6-(thiophen-2-yl)-1,2-dihydro-1,8-naphthyridine-3-carboxamide (20-trans) and **cis-1-(4-Fluorobenzyl)-N-(4-methylcyclohexyl)-2-oxo-6-(thiophen-2-yl)-1,2-dihydro-1,8-naphthyridine-3-carboxamide (20-cis).** Compounds 20-trans and 20-cis were obtained from derivative 20 by flash chromatography on a silica gel (toluene/ethyl acetate 8:1).

20-trans. Yield 24%; MS 475 m/z (M^+); mp 169–171 °C. 1H NMR ($CDCl_3$): δ 9.47 (m, 1H, NH); 8.97 (m, 2H, Ar); 8.22 (s, 1H, Ar); 7.46 (m, 3H, Ar); 7.19 (m, 2H, Ar); 6.96 (m, 2H, Ar); 5.79 (s, 2H, CH_2), 3.97 (m, 1H, CH); 1.80–0.92 (m, 12H, cyclohexyl + CH_3). ^{13}C NMR ($CDCl_3$): δ 164.39, 162.75, 162.12, 150.90, 142.47, 140.56, 138.85, 134.66, 133.26, 128.86, 127.92, 127.63, 125.56, 124.55, 122.8, 116.33, 115.28, 55.78, 46.16, 44.88, 33.25, 31.28, 29.86, 21.80.

20-cis. Yield 21%; MS 475 m/z (M^+); mp 163–165 °C. 1H NMR ($CDCl_3$): δ 9.47 (m, 1H, NH); 8.97 (m, 2H, Ar); 8.22 (s, 1H, Ar); 7.46 (m, 3H, Ar); 7.19 (m, 2H, Ar); 6.96 (m, 2H, Ar); 5.79 (s, 2H, CH_2), 3.97 (m, 1H, CH); 1.80–0.92 (m, 12H, cyclohexyl + CH_3). ^{13}C NMR ($CDCl_3$): δ 164.39, 162.75, 162.12, 150.90, 142.47, 140.56, 138.85, 134.66, 133.26, 128.86, 127.92, 127.63, 125.56, 124.55, 122.8, 116.33, 115.28, 55.78, 49.47, 44.88, 34.21, 32.20, 30.54, 22.56.

1-(4-Fluorobenzyl)-6-(4-fluorophenyl)-N-(4-methylcyclohexyl)-2-oxo-1,2-dihydro-1,8-naphthyridine-3-carboxamide (21). Purified by flash chromatography (toluene/ethyl acetate 9:1). Yield 94%; MS 487 m/z (M^+). 1H NMR ($CDCl_3$): δ 10.01 and 9.59 (2m, 1H, NH); 8.91 (m, 2H, Ar); 8.18 (s, 1H, Ar); 7.56 (m, 3H, Ar); 7.21 (m, 2H, Ar); 6.97 (m, 2H, Ar); 5.81 (s, 2H, CH_2), 4.26 and 3.92 (2m, 1H, CH); 1.82–0.92 (m, 12H, cyclohexyl + CH_3). ^{13}C NMR ($CDCl_3$): δ 164.82, 162.72, 162.14, 161.87, 150.70, 149.24, 142.55, 140.65, 139.67, 136.26, 132.55, 130.42, 129.16, 124.27, 116.88, 115.69, 115.29, 49.47, 46.16, 44.88, 34.21, 33.25, 32.20, 31.28, 30.54, 29.86, 22.56, 21.80. HRMS-ESI: m/z calcd for $C_{29}H_{27}F_2N_3O_2$ [$M+H$] $^+$, 488.2150; found 488.2137.

1-(4-Fluorobenzyl)-6-(furan-2-yl)-N-(4-methylcyclohexyl)-2-oxo-1,2-dihydro-1,8-naphthyridine-3-carboxamide (22). Purified by flash chromatography (toluene/ethyl acetate 8:1). Yield 78%. 1H NMR ($CDCl_3$): δ 9.99 and 9.60 (2m, 1H, NH); 8.98 (m, 2H, Ar); 8.29 (s, 1H, Ar); 7.49 (m, 3H, Ar); 6.99 (m, 2H, Ar); 6.80 (d, $J = 3.2$ Hz, 1H, Ar); 6.56 (m, 1H, Ar); 5.79 (s, 2H, CH_2), 4.27 and 3.93 (2m, 1H, CH); 1.83–0.91 (m, 12H, cyclohexyl + CH_3). ^{13}C NMR ($CDCl_3$): δ 164.39, 162.75, 162.12, 154.33, 150.90, 142.47, 142.09, 140.56, 134.66, 133.26, 128.86, 124.55, 122.8, 116.33, 115.28, 109.35, 107.89, 49.40, 46.26, 44.88, 34.31, 33.28, 32.00, 31.78, 30.24, 29.67, 22.50, 21.76. HRMS-ESI: m/z calcd for $C_{27}H_{26}FN_3O_3$ [$M+H$] $^+$, 460.2036; found 460.2023.

trans-1-(4-Fluorobenzyl)-6-(furan-2-yl)-N-(4-methylcyclohexyl)-2-oxo-1,2-dihydro-1,8-naphthyridine-3-carboxamide (22-trans) and **cis-1-(4-Fluorobenzyl)-6-(furan-2-yl)-N-(4-methylcyclohexyl)-2-oxo-1,2-dihydro-1,8-naphthyridine-3-carboxamide (22-cis).** Compounds 22-trans and 22-cis were obtained from derivative 22 by flash chromatography on a silica gel (toluene/ethyl acetate 8:1).

22-trans. Yield 33%; MS 459 m/z (M^+); mp 175–178 °C. 1H NMR ($CDCl_3$): δ 9.60 (m, 1H, NH); 8.98 (m, 2H, Ar); 8.29 (s, 1H, Ar); 7.49 (m, 3H, Ar); 6.99 (m, 2H, Ar); 6.80 (d, $J = 3.2$ Hz, 1H, Ar); 6.56 (m, 1H, Ar); 5.79 (s, 2H, CH_2), 3.93 (m, 1H, CH); 1.83–0.91 (m, 12H, cyclohexyl + CH_3). ^{13}C NMR ($CDCl_3$): δ 164.39, 162.75, 162.12, 154.33, 150.90, 142.47, 142.09, 140.56, 134.66, 133.26, 128.86, 124.55, 122.8, 116.33, 115.28, 109.35, 107.89, 46.26, 44.88, 33.28, 31.78, 29.67, 21.76.

22-cis. Yield 27%; MS 459 m/z (M^+); mp 168–170 °C. 1H NMR ($CDCl_3$): δ 9.99 (m, 1H, NH); 8.98 (m, 2H, Ar); 8.29 (m, 1H, Ar); 7.49 (m, 3H, Ar); 6.99 (m, 2H, Ar); 6.80 (d, $J = 3.2$ Hz, 1H, Ar); 6.56 (m, 1H, Ar); 5.79 (s, 2H, CH_2), 4.27 (m, 1H, CH); 1.83–0.91 (m, 12H, cyclohexyl + CH_3). ^{13}C NMR ($CDCl_3$): δ 164.39, 162.75, 162.12, 154.33, 150.90, 142.47, 142.09, 140.56, 134.66, 133.26, 128.86, 124.55, 122.8, 116.33, 115.28, 109.35, 107.89, 49.40, 44.88, 34.31, 32.00, 30.24, 22.50.

6-(4-Methoxyphenyl)-N-(4-methylcyclohexyl)-1-(2-morpholinoethyl)-2-oxo-1,2-dihydro-1,8-naphthyridine-3-carboxamide (23). Purified by flash chromatography (hexane/ethyl acetate 2:1). Yield 48%; MS 504 m/z (M^+). 1H NMR ($CDCl_3$): δ 10.04 and 9.63 (2m, 1H, NH); 8.90 (m, 2H, Ar); 8.18 (s, 1H, Ar); 7.56 (m, 2H, Ar); 7.06 (m, 2H, Ar); 4.77 (t, $J = 6.7$ Hz, 2H, CH_2), 4.22 and 3.96 (2m, 1H, CH); 3.89 (s, 3H, CH_3); 3.68 (m, 4H, morpholine); 2.73 (m, 6H, morpholine + CH_2); 1.95–0.87 (m, 12H, cyclohexyl + CH_3). ^{13}C NMR ($CDCl_3$): δ 162.45, 161.87, 161.06, 152.45, 148.89, 139.93, 128.72, 128.57, 125.98, 124.45, 116.31, 115.36, 114.81, 67.44, 56.34, 55.91, 54.32, 49.63, 45.82, 39.60, 34.16, 33.12, 32.25, 31.34, 30.41, 29.90, 22.43, 21.78. HRMS-ESI: m/z calcd for $C_{29}H_{36}N_4O_4$ [$M+H$] $^+$, 505.2815; found 505.2801.

N-(4-Methylcyclohexyl)-1-(2-morpholinoethyl)-2-oxo-6-(thiophen-2-yl)-1,2-dihydro-1,8-naphthyridine-3-carboxamide (24). Purified by flash chromatography (hexane/ethyl acetate 2:1). Yield 78%; MS 480 m/z (M^+). 1H NMR ($CDCl_3$): δ 10.02 and 9.61 (2m, 1H, NH); 8.94 (m, 2H, Ar); 8.20 (s, 1H, Ar); 7.41 (d, $J = 4.4$ Hz, 1H, Ar); 7.27–7.14 (m, 2H, Ar); 4.80 (t, $J = 6.6$ Hz, 2H, CH_2), 4.28 and 3.97 (2m, 1H, CH); 3.69 (m, 4H, morpholine); 2.74 (m, 6H, morpholine + CH_2); 1.82–0.88 (m, 12H, cyclohexyl + CH_3). ^{13}C NMR ($CDCl_3$): δ 162.45, 161.87, 152.45, 148.89, 139.93, 138.31, 127.92, 127.65, 125.53, 122.68, 124.45, 116.31, 115.36, 67.44, 56.34, 54.32, 49.63, 45.82,

39.60, 34.16, 33.12, 32.25, 31.34, 30.41, 29.90, 22.63, 21.80. HRMS-ESI: m/z calcd for $C_{26}H_{32}N_4O_3S$ [M+H]⁺, 481.2273; found 481.2270.

6-(4-Fluorophenyl)-N-(4-methylcyclohexyl)-1-(2-morpholinoethyl)-2-oxo-1,2-dihydro-1,8-naphthyridine-3-carboxamide (25). Purified by flash chromatography (hexane/ethyl acetate 1:1). Yield 53%; MS 492 m/z (M⁺). ¹H NMR (CDCl₃): δ 10.00 and 9.62 (2m, 1H, NH); 8.87 (m, 2H, Ar); 8.17 (s, 1H, Ar); 7.57 (m, 2H, Ar); 7.20 (m, 2H, Ar); 4.79 (t, $J = 6.6$ Hz, 2H, CH₂), 4.27 and 3.96 (2m, 1H, CH); 3.68 (m, 4H, morpholine); 2.68 (m, 6H, morpholine + CH₂); 1.80–0.89 (m, 12H, cyclohexyl + CH₃). ¹³C NMR (CDCl₃): δ 164.55, 162.24, 161.68, 152.35, 148.92, 139.88, 132.21, 129.32, 125.98, 124.65, 116.31, 116.13, 115.30, 67.48, 56.65, 54.42, 49.33, 45.75, 39.45, 34.09, 33.22, 32.64, 31.54, 30.22, 29.89, 22.64, 21.80. HRMS-ESI: m/z calcd for $C_{28}H_{33}FN_4O_3$ [M+H]⁺, 493.2615; found 493.2601.

6-(Furan-2-yl)-N-(4-methylcyclohexyl)-1-(2-morpholinoethyl)-2-oxo-1,2-dihydro-1,8-naphthyridine-3-carboxamide (26). Purified by flash chromatography (hexane/ethyl acetate 1:1). Yield 79%; MS 464 m/z (M⁺). ¹H NMR (CDCl₃): δ 10.04 and 9.64 (2m, 1H, NH); 8.99 (m, 2H, Ar); 8.28 (s, 1H, Ar); 7.57 (d, $J = 3.2$ Hz, 1H, Ar); 6.80 (d, $J = 3.2$ Hz, 1H, Ar); 6.56 (m, 1H, Ar); 4.77 (t, $J = 6.7$ Hz, 2H, CH₂), 4.22 and 3.96 (2m, 1H, CH); 3.69 (m, 4H, morpholine); 2.77 (m, 6H, morpholine + CH₂); 1.82–0.92 (m, 12H, cyclohexyl + CH₃). ¹³C NMR (CDCl₃): δ 162.31, 162.00, 152.67, 148.920, 142.77, 139.91, 124.46, 122.87, 116.33, 115.31, 109.67, 107.54, 67.68, 56.33, 54.21, 49.21, 45.65, 39.59, 34.15, 33.18, 32.57, 31.32, 30.49, 29.99, 22.63, 21.82. HRMS-ESI: m/z calcd for $C_{26}H_{32}N_4O_4$ [M+H]⁺, 465.2502; found 465.2490.

CB1 and CB2 Receptor Binding Assays. The new compounds were evaluated in CB1R and CB2R binding assays using membranes from HEK-293 cells transfected with cDNAs encoding the human recombinant CB1R ($B_{max} = 2.5$ pmol/mg protein) and human recombinant CB2R ($B_{max} = 4.7$ pmol/mg protein) (Perkin-Elmer, Italy). These membranes were incubated with [³H]-(-)-*cis*-3-[2-hydroxy-4-(1,1-dimethylheptyl)phenyl]-*trans*-4-(3-hydroxypropyl)-cyclohexanol ([³H]CP-55,940) (0.14 nM/ $K_i = 0.18$ nM and 0.084 nM/ $K_i = 0.31$ nM for CB1R and CB2R, respectively) as high-affinity ligand⁵³ and displaced with 100 nM (R)-(+)-[2,3-dihydro-5-methyl-3-(4-morpholinylmethyl)pyrrolo[1,2,3-*de*]-1,4-benzoxazin-6-yl]-1-naphthalenylmethanone (WIN-55,212-2)³⁴ as heterologous competitor for nonspecific binding ($K_i = 9.2$ and 2.1 nM, respectively, for CB1R and CB2R). All compounds were tested following the procedure described by the cell membrane manufacturer.⁵⁵

CB1R binding protocol involves the use of the same solution buffer used for both incubation and washing reaction (Tris-HCl, 50 mM; EDTA, 2.5 mM; MgCl₂, 2.5 mM; BSA, 0.5 mg/mL at pH 7.4), 0.4 nM for [³H]CP-55,940, test compounds (concentrations from 0.001 to 10 μ M), and finally 8 μ g/sample membrane in a total volume of 200 μ L. CB2R binding assays were carried out with two different buffers: incubation buffer (Tris-HCl, 50 mM; EGTA, 2.5 mM; MgCl₂, 5 mM; BSA, 1 mg/mL at pH 7.4) and washing buffer (Tris-HCl, 50 mM; EGTA, 2.5 mM; MgCl₂, 5 mM; BSA, 2% at pH 7.4). The assay mixture contained incubation buffer, 0.4 nM [³H]CP-55,940, test substances (concentrations from 0.001 to 10 μ M), and 4 μ g/sample membrane in a total assay volume of 600 μ L. Assay tubes were prepared in duplicate and incubated for 90 min at 30 °C. The reaction was terminated by addition of ice-cold buffer followed by rapid filtration under vacuum through Whatman GF/C filters (pretreated for 2 h with 0.05% aqueous polyethyleneimine) using a 12-well harvester from Millipore. After washing, radioactivity associated with the filters was counted on a liquid scintillation analyzer (Tri-Carb 2100 TR, Perkin-Elmer). Specific binding was determined by subtracting nonspecific binding from total binding in the absence of competing ligand. The percentage displacement of specific binding was calculated for the amount of radiolabel bound in the presence of unlabeled displacing ligand. Displacement IC₅₀ values were determined by linear regression analysis of log concentration–percent displacement data using GraphPad Prism. K_i values were calculated by applying the Cheng–Prusoff equation, $K_i = IC_{50}/(1 + L/K_D)$, where L is the concentration of the radioligand, IC_{50} is the concentration of drug causing 50% inhibition of specific radioligand binding, and K_D is the

dissociation constant of the radioligand–receptor complex. Data are the mean \pm SEM of at least $n = 3$ experiments.³⁶

Cell Line. U2OS cells (osteosarcoma cell line) permanently expressing *h*-CB2R and β arr2-GFP (green fluorescent protein) were obtained from Drs. Larry Barak and Marc Caron (Duke University). They were maintained at 37 °C in a humidified atmosphere containing 5% CO₂ in Dulbecco's modified Eagle medium nutrient mixture F-12 HAM, supplemented with 10% fetal bovine serum, 0.6% zeocin, and 400 mg/mL of G418. Cells were then harvested using trypsin-EDTA (Gibco catalog number 25300-054), and viable cells were assessed using trypan blue dye exclusion.

β -Arrestin Assay. The assays were performed using a procedure described previously.²² U2OS cells permanently expressing *h*-CB2R and β arr2-GFP were detached using trypsin-EDTA, seeded onto glass coverslips at 80–85% confluence, and placed in 24-well plates (BD Falcon). After incubation at 37 °C (5% CO₂, 95% relative humidity) overnight, cells were washed with Hanks's balanced salt solution (HBSS) before drug application. Test compounds and reference cannabinoid compounds were dissolved in DMSO, and dilutions were made in HBSS. In order to detect agonist-stimulated redistribution of β arr2-GFP, the cells were stimulated with various concentrations drug at room temperature for 40 min. Then the suspension was removed, paraformaldehyde (4% in HBSS, p/v) was added, and the incubation continued at room temperature for 25 min. Finally the cells were washed with PBS three times and once with double-distilled water. The antagonism protocol included 15 min of pre-incubation with the antagonist, followed by a 40 min co-incubation of antagonist and agonist (30 nM WIN-55,212-2). Glass coverslips were mounted onto slides and imaged using a fluorescence microscope (Nikon E1000; Tokyo, Japan) using a 40 \times oil objective and 488 nm excitation for GFP. The redistribution of diffuse β -arrestin-GFP from the cytoplasm to agonist- or antagonist-occupied receptor-containing pits or vesicles was imaged using a fluorescence microscope (Nikon E1000; using a 40 \times oil objective and 488 nm excitation for GFP, Tokyo, Japan). The RGB color images captured from the fluorescent microscope were transformed into 8-bit gray-scale images using the Automate-Batch function in Adobe Photoshop CSS. To quantify β arr2-GFP aggregates, gray-scale images were processed through ImageJ software (<http://rsbweb.nih.gov/ij/>), using a custom-written plug-in provided by Pingwei Zhao (Temple University). Curves were fit by nonlinear regression using the sigmoidal dose–response equation in GraphPad Prism Version 5.0 (GraphPad, San Diego, CA). Activity values were normalized to the agonist's response (30 nM WIN-55,212-2 was considered as 100%).

cAMP Assay. These assays were performed using LANCE Ultra cAMP kit (catalog number TRF0262; Perkin-Elmer Inc., Boston, MA) according to the manufacturer's protocol.

U2OS cells expressing the *h*CB2R were detached using trypsin-EDTA, washed with HBSS, and counted, and cell viability was determined using Trypan Blue stain. Cells were resuspended in stimulation buffer (HBSS, 1X; BSA stabilizer, 0.1%; IBMX, 0.5 mM; HEPES, 5 mM; pH 7.4) at a concentration of 600 cells/ μ L. In order to detect the agonist-induced reduction in cAMP levels, 5 μ L of the cell suspension (3000 cells/well) was stimulated with forskolin (10 μ M final concentration) and with various concentrations of test ligands in white Optiplate-384 wells at room temperature for 30 min. Functional antagonism of the cannabinoid CB2R antagonist response was measured by incubating the suspension cells with drug dilutions, forskolin (10 μ M final concentration), and the reference agonist WIN-55,212-2 (30 nM final concentration) at room temperature for 30 min. After the incubation, 5 μ L of europium chelated labeled cAMP tracer solution in detection buffer and then 5 μ L of the cAMP-specific monoclonal antibodies (labeled with ULight-dye) solution in detection buffer were added to the wells. The reaction was allowed to incubate for 1 h at room temperature in the dark. Time-resolved fluorescence signals were detected on an EnVision multiplate reader (Perkin-Elmer, CA, USA) at 615 and 665 nm emission. The amounts of cAMP produced in the stimulated cells were determined according to the cAMP standard curves. Antagonism in the cAMP assay has been expressed as percent of inhibition of WIN-55,212-2. Inhibition curves

were analyzed by nonlinear regression using GraphPad Prism Version 5.0 software (GraphPad, San Diego, CA), and data were fitted to sigmoidal concentration–response curves to obtain IC_{50} values. Also for agonist, the sigmoidal dose–response equation was used to determine EC_{50} values. In this case, the logarithmic value of agonist concentrations is plotted against the TR-FRET signal normalized to the response of forskolin.

Ballesteros–Weinstein Nomenclature. Here, the Ballesteros–Weinstein numbering system for GPCR amino acid residues is used. In this numbering system, the label 0.50 is assigned to the most highly conserved Class A residue in each transmembrane helix (TMH).³⁷ This is preceded by the TMH number. In this system, for example, the most highly conserved residue in TMH6 is P6.50. The residue immediately before this would be labeled 6.49, and the residue immediately after this would be labeled 6.51. When referring to a specific CB2 residue, the Ballesteros–Weinstein name is followed by the absolute sequence number given in parentheses (e.g., K3.28(109)); however, when referring to a highly conserved residue among Class A GPCRs (and not a specific residue in CB2), only the Ballesteros–Weinstein name is given.

Modeling Methods. Conformational Search. The structures of ligands were built in Spartan'08 (Wave function, Inc., Irvine, CA). Initial conformational analyses of these compounds were performed using the semiempirical method AM1 encoded in Spartan'08. Conformational searches were performed (using 3–8-fold rotations) for each rotatable bond. All unique conformers identified were then optimized with *ab initio* Hartree–Fock calculations at the 6-31G* level, except for **17** and **18**, which required 6-311G* to accommodate a bromine atom. To calculate the difference in energy between the global minimum energy conformer of each compound and its final docked conformation, rotatable bonds in the global minimum energy conformer were driven to their corresponding value in the final docked conformation, and the single-point energy of the resultant structure was calculated at the HF 6-31G* level, or for **17** and **18** at the 6-311G* level.

Model Development. Complete details on the generation of the inactive and activated state CB2R models used here are available in our previous publication.³¹ We provide a synopsis below.

CB2R Inactive State Model. The crystal structure of the Class A GPCR, rhodopsin in the dark state was used as the template for the creation of our CB2R inactive state model.²⁶ This template was chosen because no mutations or modifications were made to its structure for crystallization. In addition, the cannabinoid receptors and rhodopsin share some unusual sequence motifs. These receptors share a TMH4 GWNC motif at their extracellular ends. Here a TRP forms an aromatic stacking interaction with Y5.39, influencing the EC positions of TMH3–4–5. The initial homology model was refined by calculating the low free energy conformations for any TMH with an important sequence divergence from rhodopsin and replacing the corresponding helix from the initial model with one that more accurately reflects the sequence dictated TMH geometries in CB2R. This includes TMH2 (GG helix distorting motif in Rho vs no PRO or GG in CB2R) and TMH5 (PRO at 5.50 in Rho vs no PRO at 5.50 in CB2R). The resultant CB2R model has been tested using results from substituted cysteine accessibility studies to identify binding pocket facing residues,^{38,39} from mutation studies of key ligand interactions sites,^{38–41} and from covalent labeling studies of CB2R⁴² that support a lipid entry pathway for CB2R ligands.

To permit adjustment to a lipid bilayer environment, the resultant model was pre-equilibrated in a stearyl-docosahexaenoylphosphatidylcholine (SDPC) bilayer for 300 ns.³¹ While the toggle switch residue, W6.48(258), remained in its inactive state g^+ χ^1 dihedral angle after the equilibration in SDPC, some notable changes did occur during this equilibration. The R3.50(131) and D6.30(240) salt bridge at the intracellular ends of TMHs3/6 (analogous to the R3.50(135)/E6.30(247) salt bridge in the dark state of rhodopsin) rearranged quickly to form a salt bridge between R3.55(136) and D6.30(240), with Y3.51(132) supporting the salt bridge by hydrogen bonding to the exposed backbone carbonyl of L6.29(239). A second notable

change was the development of additional helical turns in the IC-3 (TMH5–TMH6) loop after the original end of TMH5.³¹

CB2R Activated State Model. The CB2R activated state model (R*) used here for docking studies was produced from the inactive state model described above via a multimicrosecond-long molecular dynamics simulation of the interaction of the endogenous CB2R ligand, 2-AG, with CB2R in a palmitoyl-oleoyl-phosphatidylcholine (POPC) bilayer. In these simulations, 2-AG entered the binding pocket via the lipid bilayer between TMH6 and TMH7 and activated the CB2R. Ligand entry resulted in changes on the intracellular end of the receptor. Here the R3.55(136)/D6.30(240) ionic lock was broken as TMH6 straightened and moved its IC end away from the TMH bundle. Ligand entry also resulted in changes in the binding pocket, as toggle switch residue W6.48(258) underwent a χ^1 torsion angle change from g^+ to *trans*. This change was transitory, with W6.48(258) reverting to a g^+ χ^1 . The R* model used for docking studies here was taken from the section of the trajectory in which the W6.48(258) χ^1 was *trans*.³¹

Ligand/CB2R Complexes. The inactive state model was used to dock compounds **17**, **18**, and **23**, while **A1**, **A2**, **5**, and **14** were docked in the activated state model described above. In addition, to probe the origins of the antagonism vs agonism of **23** and **A1**, each compound was docked in our CB2R inactive state model. The automatic docking program Glide v5.8 (Schrodinger Inc., Portland, OR) was used to explore possible binding conformations or receptor site interactions with flexible docking.^{31,32} Because S7.39(285) has been shown to be a ligand interaction site in CB2R,³⁷ S7.39(285) was defined as a required interaction during the initial flexible docking procedure. Glide was used to generate a grid based on the centroid of the ligand in the binding site. Any hydrophobic region defined in the grid generation that contacted the ligand was selected as important to the flexible docking procedure. The box for flexible docking was defined to be 26 Å in the *x*, *y*, and *z* dimensions. Extra precision (XP) was selected with scaling of VdW radii and flexible docking invoked.³⁴ These Glide docking studies consistently identified an interaction with K3.28(109). A second Glide docking study was initiated in which K3.28(109) and S7.39(285) were defined as required interactions during the flexible docking procedure. Extra precision (XP) was selected and flexible docking invoked. This second run resulted in improved Glide scores, particularly for ligands with higher CB2R binding affinities.

For each receptor–ligand complex, the complex with the best Glide score was minimized using the OPLS2005 all-atom force field in Macromodel 9.9 (Schrodinger Inc.). An 8.0 Å nonbonded cutoff (updated every 10 steps), a 20.0 Å electrostatic cutoff, and a 4.0 Å hydrogen bond cutoff were used in each stage of the calculation. The first stage consisted of 3500 steps of Polak–Ribier conjugate gradient minimization using a distance-dependent dielectric function with a base constant of 2. No harmonic constraints were placed on the side chains, but 100 kJ/mol torsional constraints were applied to hold all the backbone ϕ/ψ torsion angles. During the second stage of 500 steps, all torsional constraints were released. To relax the loops, an additional 1000-step Polak–Ribier conjugate gradient minimization of the loop regions was performed. The loop and termini regions were left free, while the transmembrane regions were not allowed to move during this final minimization. An 8.0 Å extended nonbonded cutoff (updated every 10 steps), 20.0 Å electrostatic cutoff, and 4.0 Å hydrogen bond cutoff were used in this calculation, and the generalized Born/surface area (GB/SA) continuum solvation model for water available in Macromodel was employed.

■ ASSOCIATED CONTENT

Supporting Information

Table T1, dihedral definitions of the global minima energy conformers of **17**, **18**, **23**, **A1**, **A2**, **14**, and **5**; Table T2, energetic cost of docked ligand conformations; Tables T3 and T4, hydrogen bond parameters between each compound and K3.28(109) and S7.39(285), respectively; Table T5, ligand–receptor aromatic stacking interactions; Figure S1, drawings of the 1,8-naphthyridine scaffolds; Figures S2 and S3, global

minima for antagonists **17**, **18**, and **23** and for agonists **A1**, **A2**, **5**, and **14**, respectively; discussion of ligand/receptor complexes, including detailed description of the binding pocket interactions; Figures S4 and S5, models of the antagonists/inverse agonists **17**, **18**, and **23** docked in CB2R (inactive) and of the agonists **A1**, **A2**, **14**, and **5** docked in CB2R* (active), respectively; Figure S6, spatial relationship between compound **17** and the toggle switch residue W6.48(258). This material is available free of charge via the Internet at <http://pubs.acs.org>.

AUTHOR INFORMATION

Corresponding Authors

*P.H.R.: phone, (336) 334-5333; e-mail, phreggio@uncg.edu.

*C.M.: phone, +39(0)502219548; e-mail, clementina.manera@farm.unipi.it.

Notes

The authors declare no competing financial interest.

ACKNOWLEDGMENTS

This work was supported by NIH grants RO1 DA003934 and KOS DA021359 (PHR), R01 DA023204 and P30 DA013429, and by National Interest Research Projects (PRIN 2010-2011, Grant 20105YY2HL_008).

REFERENCES

- (1) Velasco, G.; Sanchez, C.; Guzman, M. Towards the use of cannabinoids as antitumour agents. *Nat. Rev. Cancer* **2012**, *12*, 436–444.
- (2) Pertwee, R. G. Targeting the endocannabinoid system with cannabinoid receptor agonists: pharmacological strategies and therapeutic possibilities. *Philos. Trans. R. Soc. London B Biol. Sci.* **2012**, *367*, 3353–3363.
- (3) Gaoni, Y.; Mechoulam, R. Isolation, Structure, and Partial Synthesis of an Active Constituent of Hashish. *J. Am. Chem. Soc.* **1964**, *86*, 1646–1647.
- (4) Matsuda, L. A.; Lolait, S. J.; Brownstein, M. J.; Young, A. C.; Bonner, T. I. Structure of a cannabinoid receptor and functional expression of the cloned cDNA. *Nature* **1990**, *346*, 561–564.
- (5) Munro, S.; Thomas, K. L.; Abu-Shaar, M. Molecular characterization of a peripheral receptor for cannabinoids. *Nature* **1993**, *365*, 61–65.
- (6) Ameri, A. The effects of cannabinoids on the brain. *Prog. Neurobiol.* **1999**, *58*, 315–348.
- (7) Das, S. K.; Paria, B. C.; Chakraborty, I.; Dey, S. K. Cannabinoid ligand-receptor signaling in the mouse uterus. *Proc. Natl. Acad. Sci. U.S.A.* **1995**, *92*, 4332–4336.
- (8) Galiegue, S.; Mary, S.; Marchand, J.; Dussossoy, D.; Carriere, D.; Carayon, P.; Bouaboula, M.; Shire, D.; Le Fur, G.; Casellas, P. Expression of central and peripheral cannabinoid receptors in human immune tissues and leukocyte subpopulations. *Eur. J. Biochem.* **1995**, *232*, 54–61.
- (9) Gerard, C. M.; Mollereau, C.; Vassart, G.; Parmentier, M. Molecular cloning of a human cannabinoid receptor which is also expressed in testis. *Biochem. J.* **1991**, *279* (Pt 1), 129–134.
- (10) Wenger, T.; Ledent, C.; Csernus, V.; Gerendai, I. The central cannabinoid receptor inactivation suppresses endocrine reproductive functions. *Biochem. Biophys. Res. Commun.* **2001**, *284*, 363–368.
- (11) Onaivi, E. S.; Ishiguro, H.; Gong, J. P.; Patel, S.; Perchuk, A.; Meozzi, P. A.; Myers, L.; Mora, Z.; Tagliaferro, P.; Gardner, E.; Brusco, A.; Akinshola, B. E.; Liu, Q. R.; Hope, B.; Iwasaki, S.; Arinami, T.; Teasensfitz, L.; Uhl, G. R. Discovery of the presence and functional expression of cannabinoid CB2 receptors in brain. *Ann. N.Y. Acad. Sci.* **2006**, *1074*, 514–36.
- (12) Battista, N.; Di Tommaso, M.; Bari, M.; Maccarrone, M. The endocannabinoid system: an overview. *Front. Behav. Neurosci.* **2012**, *6*, 1–7.
- (13) Benito, C.; Nunez, E.; Tolon, R. M.; Carrier, E. J.; Rabano, A.; Hillard, C. J.; Romero, J. Cannabinoid CB2 receptors and fatty acid amide hydrolase are selectively overexpressed in neuritic plaque-associated glia in Alzheimer's disease brains. *J. Neurosci.* **2003**, *23*, 11136–11141.
- (14) Cabral, G. A.; Marciano-Cabral, F. Cannabinoid receptors in microglia of the central nervous system: immune functional relevance. *J. Leukoc. Biol.* **2005**, *78*, 1192–1197.
- (15) Carlisle, S. J.; Marciano-Cabral, F.; Staab, A.; Ludwick, C.; Cabral, G. A. Differential expression of the CB2 cannabinoid receptor by rodent macrophages and macrophage-like cells in relation to cell activation. *Int. Immunopharmacol.* **2002**, *2*, 69–82.
- (16) Onaivi, E. S.; Ishiguro, H.; Gong, J. P.; Patel, S.; Meozzi, P. A.; Myers, L.; Perchuk, A.; Mora, Z.; Tagliaferro, P. A.; Gardner, E.; Brusco, A.; Akinshola, B. E.; Liu, Q. R.; Chirwa, S. S.; Hope, B.; Lujilde, J.; Inada, T.; Iwasaki, S.; Macharia, D.; Teasensfitz, L.; Arinami, T.; Uhl, G. R. Functional expression of brain neuronal CB2 cannabinoid receptors are involved in the effects of drugs of abuse and in depression. *Ann. N.Y. Acad. Sci.* **2008**, *1139*, 434–449.
- (17) Roche, M.; Finn, D. P. Brain CB2 Receptors: Implications for Neuropsychiatric Disorders. *Pharmaceuticals* **2010**, *3*, 2517–2553.
- (18) Cianchi, F.; Papucci, L.; Schiavone, N.; Lulli, M.; Magnelli, L.; Vinci, M. C.; Messerini, L.; Manera, C.; Ronconi, E.; Romagnani, P.; Donnini, M.; Perigli, G.; Trallori, G.; Tanganelli, E.; Capaccioli, S.; Masini, E. Cannabinoid receptor activation induces apoptosis through tumor necrosis factor alpha-mediated ceramide de novo synthesis in colon cancer cells. *Clin. Cancer. Res.* **2008**, *14*, 7691–7700.
- (19) Manera, C.; Saccomanni, G.; Adinolfi, B.; Benetti, V.; Ligresti, A.; Cascio, M. G.; Tuccinardi, T.; Lucchesi, V.; Martinelli, A.; Nieri, P.; Masini, E.; Di Marzo, V.; Ferrarini, P. L. Rational design, synthesis, and pharmacological properties of new 1,8-naphthyridin-2(1H)-on-3-carboxamide derivatives as highly selective cannabinoid-2 receptor agonists. *J. Med. Chem.* **2009**, *52*, 3644–3651.
- (20) Rinaldi-Carmona, M.; Barth, F.; Millan, J.; Derocq, J. M.; Casellas, P.; Congy, C.; Oustric, D.; Sarran, M.; Bouaboula, M.; Calandra, B.; Portier, M.; Shire, D.; Breliere, J. C.; Le Fur, G. L. SR 144528, the first potent and selective antagonist of the CB2 cannabinoid receptor. *J. Pharmacol. Exp. Ther.* **1998**, *284*, 644–650.
- (21) Huffman, J. W.; Liddle, J.; Yu, S.; Aung, M. M.; Abood, M. E.; Wiley, J. L.; Martin, B. R. 3-(1',1'-Dimethylbutyl)-1-deoxy-delta8-THC and related compounds: synthesis of selective ligands for the CB2 receptor. *Bioorg. Med. Chem.* **1999**, *7*, 2905–2914.
- (22) Sharir, H.; Console-Bram, L.; Mundy, C.; Popoff, S. N.; Kapur, A.; Abood, M. E. The endocannabinoids anandamide and virodhamine modulate the activity of the candidate cannabinoid receptor GPR55. *J. Neuroimmune Pharmacol.* **2012**, *7*, 856–865.
- (23) Manera, C.; Saccomanni, G.; Malfitano, A. M.; Bertini, S.; Castelli, F.; Laezza, C.; Ligresti, A.; Lucchesi, V.; Tuccinardi, T.; Rizzolio, F.; Bifulco, M.; Di Marzo, V.; Giordano, A.; Macchia, M.; Martinelli, A. Rational design, synthesis and anti-proliferative properties of new CB2 selective cannabinoid receptor ligands: an investigation of the 1,8-naphthyridin-2(1H)-one scaffold. *Eur. J. Med. Chem.* **2012**, *52*, 284–294.
- (24) Li, J.; Edwards, P. C.; Burghammer, M.; Villa, C.; Schertler, G. F. Structure of bovine rhodopsin in a trigonal crystal form. *J. Mol. Biol.* **2004**, *343*, 1409–1438.
- (25) Okada, T.; Fujiyoshi, Y.; Silow, M.; Navarro, J.; Landau, E. M.; Shichida, Y. Functional role of internal water molecules in rhodopsin revealed by X-ray crystallography. *Proc. Natl. Acad. Sci. U.S.A.* **2002**, *99*, 5982–5987.
- (26) Palczewski, K.; Kumasaka, T.; Hori, T.; Behnke, C. A.; Motoshima, H.; Fox, B. A.; Le Trong, I.; Teller, D. C.; Okada, T.; Stenkamp, R. E.; Yamamoto, M.; Miyano, M. Crystal structure of rhodopsin: A G protein-coupled receptor. *Science* **2000**, *289*, 739–745.
- (27) Standfuss, J.; Edwards, P. C.; D'Antona, A.; Fransen, M.; Xie, G.; Oprian, D. D.; Schertler, G. F. The structural basis of agonist-induced activation in constitutively active rhodopsin. *Nature* **2011**, *471*, 656–660.

(28) McAllister, S. D.; Hurst, D. P.; Barnett-Norris, J.; Lynch, D.; Reggio, P. H.; Abood, M. E. Structural mimicry in class A G protein-coupled receptor rotamer toggle switches: the importance of the F3.36(201)/W6.48(357) interaction in cannabinoid CB1 receptor activation. *J. Biol. Chem.* **2004**, *279*, 48024–48037.

(29) McAllister, S. D.; Rizvi, G.; Anavi-Goffer, S.; Hurst, D. P.; Barnett-Norris, J.; Lynch, D. L.; Reggio, P. H.; Abood, M. E. An Aromatic Microdomain at the Cannabinoid CB(1) Receptor Constitutes an Agonist/Inverse Agonist Binding Region. *J. Med. Chem.* **2003**, *46*, 5139–5152.

(30) Choe, H. W.; Kim, Y. J.; Park, J. H.; Morizumi, T.; Pai, E. F.; Krauss, N.; Hofmann, K. P.; Scheerer, P.; Ernst, O. P. Crystal structure of metarhodopsin II. *Nature* **2011**, *471*, 651–655.

(31) Hurst, D. P.; Grossfield, A.; Lynch, D. L.; Feller, S.; Romo, T. D.; Gawrisch, K.; Pitman, M. C.; Reggio, P. H. A lipid pathway for ligand binding is necessary for a cannabinoid G protein-coupled receptor. *J. Biol. Chem.* **2010**, *285*, 17954–17964.

(32) Kobilka, B. K.; Deupi, X. Conformational complexity of G-protein-coupled receptors. *Trends Pharmacol. Sci.* **2007**, *28*, 397–406.

(33) Gatley, S. J.; Lan, R.; Pyatt, B.; Gifford, A. N.; Volkow, N. D.; Makriyannis, A. Binding of the non-classical cannabinoid CP 55,940, and the diarylpyrazole AM251 to rodent brain cannabinoid receptors. *Life Sci.* **1997**, *61* (14), PL 191–197.

(34) Huffman, J. W.; Zengin, G.; Wu, M. J.; Lu, J.; Hynd, G.; Bushell, K.; Thompson, A. L.; Bushell, S.; Tartal, C.; Hurst, D. P.; Reggio, P. H.; Selley, D. E.; Cassidy, M. P.; Wiley, J. L.; Martin, B. R. Structure-activity relationships for 1-alkyl-3-(1-naphthoyl)indoles at the cannabinoid CB(1) and CB(2) receptors: steric and electronic effects of naphthoyl substituents. New highly selective CB(2) receptor agonists. *Bioorg. Med. Chem.* **2005**, *13* (1), 89–112.

(35) Bisogno, T.; Cascio, M. G.; Saha, B.; Mahadevan, A.; Urbani, P.; Minassi, A.; Appendino, G.; Saturnino, C.; Martin, B.; Razdan, R.; Di Marzo, V. Development of the first potent and specific inhibitors of endocannabinoid biosynthesis. *Biochim. Biophys. Acta* **2006**, *1761* (2), 205–212.

(36) Cheng, Y.; Prusoff, W. H. Relationship between the inhibition constant (KI) and the concentration of inhibitor which causes 50% inhibition (I50) of an enzymatic reaction. *Biochem. Pharmacol.* **1973**, *22*, 3099–3108.

(37) Ballesteros, J. A.; Weinstein, H. Integrated methods for the construction of three-dimensional models and computational probing of structure-function relations in G protein-coupled receptors. In *Methods in Neurosciences*; Stuart, C. S., Ed.; Academic Press: San Diego, CA, 1995; Vol. 25, pp 366–428.

(38) Zhang, R.; Hurst, D. P.; Barnett-Norris, J.; Reggio, P. H.; Song, Z. H. Cysteine 2.59(89) in the Second Transmembrane Domain of Human Cb2 Receptor Is Accessible within the Ligand Binding Crevice: Evidence for Possible Cb2 Deviation from a Rhodopsin Template. *Mol. Pharmacol.* **2005**, *68*, 69–83.

(39) Song, Z. H.; Slowey, C. A.; Hurst, D. P.; Reggio, P. H. The difference between the CB(1) and CB(2) cannabinoid receptors at position 5.46 is crucial for the selectivity of WIN55212–2 for CB(2). *Mol. Pharmacol.* **1999**, *56*, 834–840.

(40) Tao, Q.; McAllister, S. D.; Andreassi, J.; Nowell, K. W.; Cabral, G. A.; Hurst, D. P.; Bachtel, K.; Ekman, M. C.; Reggio, P. H.; Abood, M. E. Role of a conserved lysine residue in the peripheral cannabinoid receptor (CB2): evidence for subtype specificity. *Mol. Pharmacol.* **1999**, *55*, 605–613.

(41) Nebane, N. M.; Hurst, D. P.; Carrasquer, C. A.; Qiao, Z.; Reggio, P. H.; Song, Z. H. Residues accessible in the binding-site crevice of transmembrane helix 6 of the CB2 cannabinoid receptor. *Biochemistry* **2008**, *47*, 13811–13821.

(42) Pei, Y.; Mercier, R. W.; Anday, J. K.; Thakur, G. A.; Zvonok, A. M.; Hurst, D.; Reggio, P. H.; Janero, D. R.; Makriyannis, A. Ligand-binding architecture of human CB2 cannabinoid receptor: evidence for receptor subtype-specific binding motif and modeling GPCR activation. *Chem. Biol.* **2008**, *15*, 1207–1219.